WINDBORNE DEBRIS MISSILE IMPACTS ON WINDOW GLAZING AND SHUTTER SYSTEMS

By

NIRAV SHAH

A THESIS PRESENTED TO THE GRADUATE SCHOOL
OF THE UNIVERSITY OF FLORIDA IN PARTIAL FULFILLMENT
OF THE REQUIREMENTS FOR THE DEGREE OF
MASTER OF SCIENCE

UNIVERSITY OF FLORIDA

2009

To my family; Mom Hema Shah, Dad Sunil Shah, and Sister Namrata Shah
For your support and encouragement in all my academic endeavors

ACKNOWLEDGMENT

I express my most sincere gratitude to my advisor and chairman of the supervisory committee, Dr. Forrest Masters, for his constant guidance, encouragement, and support. I also thank other committee members including Dr. Kurtis Gurley and Dr. David Prevatt for their assistance. I thank Dr. Jim Austin and Chuck Broward. I also appreciate friendly and helpful lab mates: George Fernandez and Jimmy Jesteadt. I am extremely grateful to my parents, Sunil Shah and Hema Shah, for their love and encouragement during my entire life. I thank my grandparents, my sister, and Amin Family for their support.

TABLE OF CONTENTS

LIST OF TABLES

LIST OF FIGURES

Abstract of Thesis Presented to the Graduate School
of the University of Florida in Partial Fulfillment of the
Requirements for the Degree of Master of Science

WINDBORNE DEBRIS MISSILE IMPACTS ON WINDOW GLAZING AND SHUTTER SYSTEMS

By

Nirav Shah

May 2009

Chair: Forrest Masters
Major: Civil Engineering

Windborne debris is a significant cause of damage to the building envelope in major hurricanes. The building envelope consists of the roof, doors, windows and cladding components of a building. The failure of the building envelope results in internal pressurization of the structure, which effectively increases the wind loads on cladding and components of building envelope and exposes the building contents to wind-driven rain.

In particular, post-hurricane investigations reports have shown that windborne debris is a significant hazard to glass during wind storms. This research aims to investigate the effects of windborne asphalt roof shingles on window glazing. Impact tests were conducted on 3.18 mm (1/8”) annealed and 4.76 mm (3/16”) annealed glass. New and old roof shingle tabs, both full weight and half weight, were considered. Two types of flight modes were considered, autorotation and tumbling. An analysis of variance (ANOVA) was performed on the experimental data to correlate glass thickness, missile weight and momentum required to break the glass.

Roofing tile or tile fragments have been also observed to damage window shutters and the glazing behind them. In this research, a second series of tests were performed to investigate the performance of window shutter systems when subjected to the impact of roofing tiles and a

standard 2x4 missile. Impact tests were performed at two different impact speeds, 20.12 m/s (45 mph) and 15.2 m/s (34 mph), and with two types of installation methods, direct mount method and tracking method. Deflections due to impact of the tile missile and 2x4 lumber were recorded and compared.

CHAPTER 1
INTRODUCTION

A breach of the building envelope can lead to a sudden increase in the net pressure acting on the roof system and expose the building contents to wind-driven rain (Lin et al, 2007; Minor, 1994). Windborne debris has been established as the principal cause of this phenomena, after the effects of Hurricane Andrew (1992); as a result, the building design process has been changed to address the debris impact on various components and cladding of the building envelope so that it maintains its integrity during extreme wind events. Modern building codes including the Florida Building Code (FBC, 2004) and International Residential Code (IRC, 2006) require that fenestration and in some cases, wall and roof claddings, be tested to certify a minimum impact strength standard to survive impacts from windborne debris when buildings are located in windborne debris regions.

The research presented here focuses on the impact of shingles on residential glazing and that of concrete tile on shutter systems. This research was performed at the request of the Hurricane Research Advisory Committee of the Florida Building Commission, which was created to address building failures resulting from the 2004 hurricanes that impacted Florida.

To complete this research it was necessary to develop two testing apparatuses. A custom shingle “launcher” was constructed to propel asphalt roof shingles with sufficient velocity to damage annealed glass specimens that varied in thickness and frontal area. Projectiles included new and naturally aged shingles of various sizes and weights. Velocity, momentum and kinetic energy of the projectile were analyzed to determine thresholds of breakage.

A second projectile “launcher” was constructed to propel concrete tiles into galvanized steel storm shutters to determine their impact resistance. Duplicate test specimens underwent a second round of testing using the large missile impact test procedures set forth in FBC 1626.2, which utilizes a piece of 2x4 timber weighing 4.1 kg (9 lb) as a representative missile.

In order to better understand the behavior of building components against missile impact during extreme wind events, it was important to understand the characteristics of fluctuating wind pressure and their effects on building envelope. The following section describes extreme wind behavior on low-rise buildings and the resulting damage due to debris impact.

1.1 Extreme Wind Effects on Low-Rise Buildings

During extreme wind events, the fluctuating pressure loading that acts on structures is caused by the mechanical turbulence created by the upwind terrain and the flow distortion created by the building. Turbulent aerodynamic wind effects include the frontal vortex, recirculation zones, shear layers, and flow separation at corners of the building (Figure 1-1). The resultant wind-structure interaction is summarized below (Yeatts and Mehta, 1993; Krishna, 1995; FEMA, 2000):

1. Positive pressures act on windward walls and windward surfaces of steep sloped roofs. The stagnation point will be found at about two-thirds of the height on the windward wall (Cook 1985). Below the stagnation point, wind flows downward and it rolls up into a vortex and travels horizontally outward across the wall.

2. Negative pressures act on leeward walls, side walls, leeward surfaces of steep sloped roofs, and all roof surfaces for low sloped roofs or steep sloped roofs when winds are parallel to the ridge. The side walls are subjected to separation flow and a reattachment flow. Wind flow separation occurs at the sharp corners and edges. This separated wind flow becomes reattached onto the surface, causing reattachment flow. Suction pressure is higher at the corners and edges, and decreases downward depending upon the length-to-width ratio of the bluff body. The leeward wall is usually exposed to the wake region. The wake region is divided into two parts – near-wake region (re-circulating flow immediately behind the building) and the far-wake region (wind flowing downstream and eventually blending with boundary layer flow). (Cook 1985). The suction pressure is generally constant on the leeward side. The pressure fluctuation on the roof is dependent on the roof’s shape, pitch and the presence of architectural features like overhangs, or parapets.

3. Windows, doors and other openings are subjected to wind pressures during extreme wind events and the impact of wind borne missiles.

The present research project focuses on the third phenomenon stated above, particularly the impact of windborne roof cover on glazing and shutter systems intended for hurricane prone regions.

1.2 Damage Due to Wind Borne Debris

The United States sustains billions of dollars per year in property and economic losses due to extreme wind events such as hurricanes, tornadoes, and winter storms, which cause damage mainly to low-rise residential structures and light commercial structures. Pielke and Landsea (1998) estimated that the average economic loss was $4.8 billion (in 1995 dollars) due to tropical cyclone impacts in United States during 1925-95.

Numerous studies of post-hurricane damage specifically cite windborne debris as a major source of damage to the building envelope. The literature on the subject becomes more abundant as Minor (1994), Beason (1984), McDonald (2000) began to record the observations during various windstorm events. They also presented a synopsis of damage observations for various hurricanes such as Celia (1970), Frederic (1979), Allen (1981), Alicia (1983), and Andrew (1992). Reed (1970) observed windborne debris as a principal source of damage to windows of high-rise buildings during the Lubbock Storm of May 11, 1970 (Minor 1994). Damage surveys conducted after Hurricane Celia (1970) revealed that the breakage of windows in downtown Corpus Christi, Texas, was mainly caused due to debris carried by wind. Pieces of roofing material, sheet metal, garbage cans and roof gravel were observed as glass-breaking agents (Minor 1994). Another notable example of windborne debris damage was in Darwin, Australia, due to Tropical Cyclone Tracy in 1974. Beason et al (1984) investigated the damage caused by Hurricane Alicia (1983) in Houston, Texas, and observed that windborne missiles from building roofs were the major cause of damage to architectural glazing systems. The investigators also concluded that building envelope failures caused by windborne debris generally occurred before lateral pressure became critical. Following Hurricane Andrew (1992), the FEMA Technical Standards Division assembled a team of engineers and architects to examine the performance of buildings in the affected area. Oliver and Hanson (1994) observed that the debris impact shattered glazing components. The investigators also observed that debris from roofing materials, especially clay and concrete roofing tile, was the most common type that caused significant damage to building envelope systems (Ayscue 1996).

After Hurricane Andrew, the 2004 and 2005 Atlantic hurricane seasons were one of the most costly hurricane seasons on record. In the investigations following Hurricane Charley (2004), researchers found that windborne missiles originated from the roofs of residential structures. Damage was observed on several asphalt shingle roofs due to the lack of bonding adhesive. The principal source of windborne debris was the blowing-off of hip or ridge shingles. Tile damage was also observed in the areas of Port Charlotte and Punta Gorda (FEMA 2005a). The blow-off of the tiles along eaves and of the hip and ridge tiles was documented by FEMA (2005a). The FEMA (FEMA 2005a) report also mentioned that tile or tile fragments easily penetrated through windows. Figure 1-3 shows the window shutter damage due to strike of tile (Reinhold 2005). In many cases windows were broken by tiles from a neighbor's house (Meloy et al. 2007). Gurley (2006) described how window performance during the 2004 storms was related to wind speed, window protection use, and the dominant roof cover type in the neighborhood. The window performance graph is shown in Figure 1-4 for properties located in the region of the 58-67 m/s (130-150 mph) wind gust during Hurricane Charley. The graph clearly indicates that even protected windows are susceptible to damage due to a tile strike. FEMA (2005b) also noted that shingles and tiles were blown off during Hurricane Ivan (2004), and they caused damage to unprotected glazing and shutters.

1.3 Thesis Summary

Chapter 2 presents background information on common windborne debris types, missile impact testing standards and previous research pertinent to this research topic. Chapter 3 presents the experimental configuration to test glazing against shingle missile impact, the apparatus and procedures used during the experiments, and the results of the experiment. Chapter 4 presents the experimental configuration to test window shutters against tile missile impact and 2x4 missile impact, the apparatus, and procedures and the results of the experiment. Chapter 5 provides the conclusions based on findings in Chapter 3 and Chapter 4. Chapter 5 makes recommendations for future research activities supporting this research.

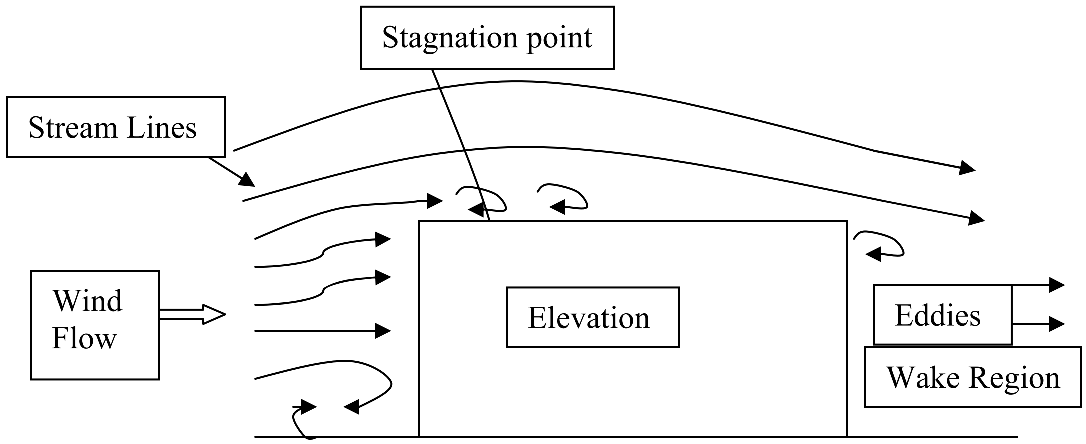

A

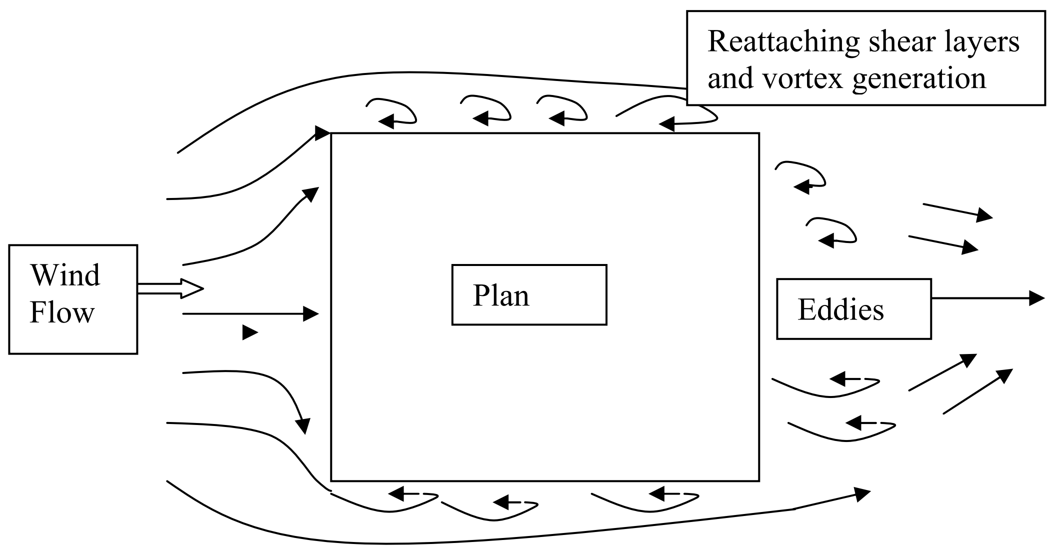

B

Figure 1-1. Wind flow around building. A) Elevation. B) Plan.

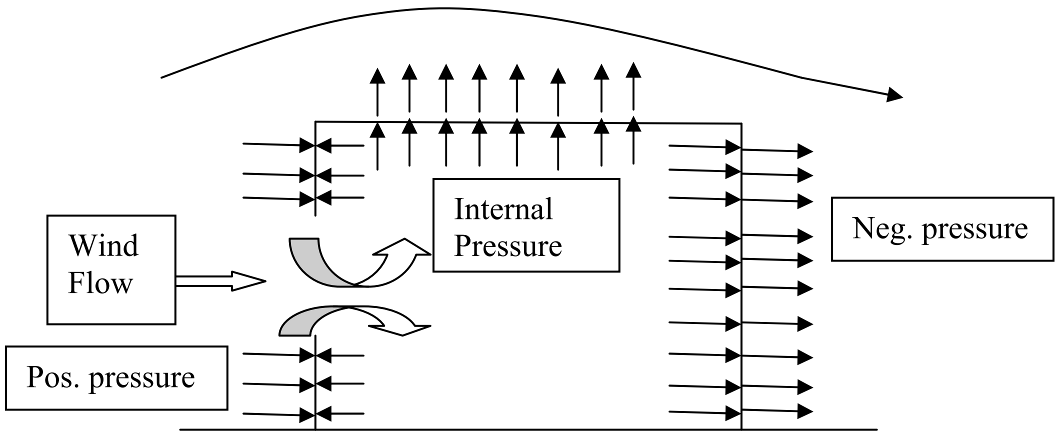

Figure 1-2. Windward wall opening caused increase in internal pressure (Side view)

Figure 1-3. Window shutter damage due to Spanish tile. (Reinhold 2005)

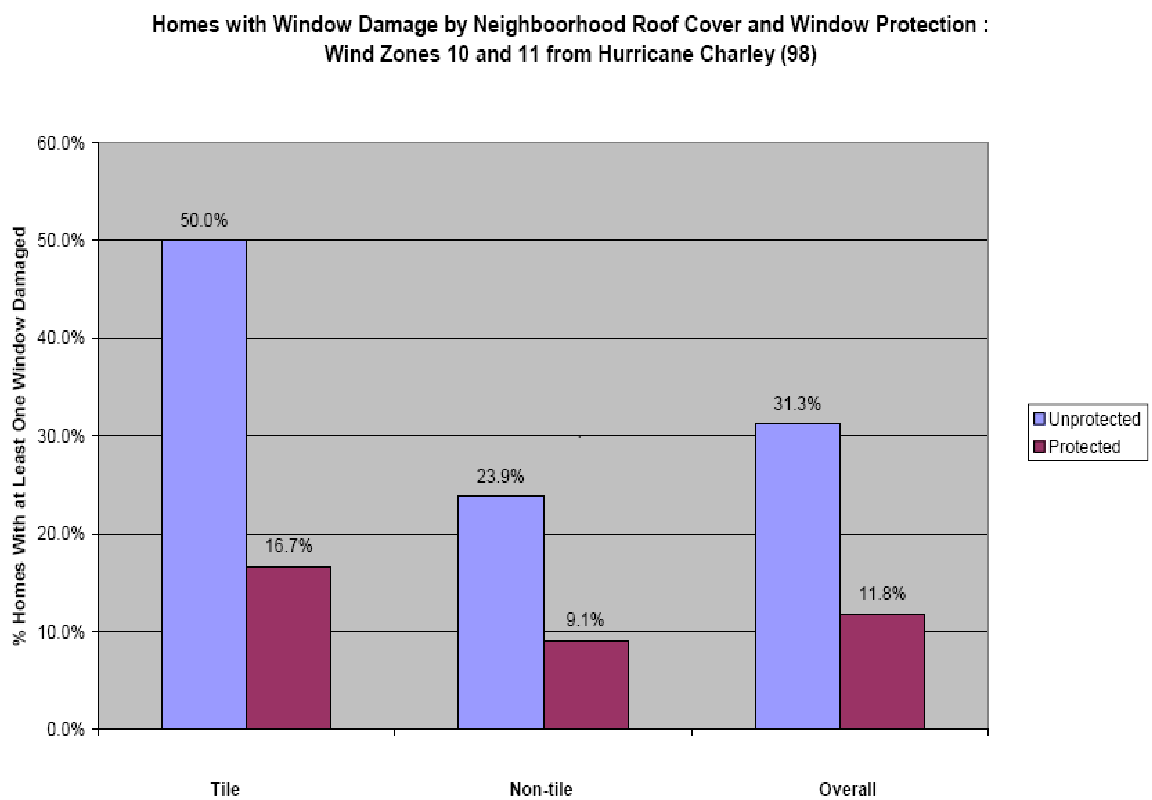

Figure 1-4. Percentage of homes with at least one window damaged as a function of neighborhood roof cover type and window protection. (Gurley 2006).

CHAPTER 2
BACKGROUND

Severe windstorm events routinely cause significant damage to the building envelope. The impacts of extreme windstorms on the existing engineering systems have invited serious attention of engineers in the last four decades. In the previous chapter, the discussion consisted of the breach of the building envelope due to impacts of windborne debris. Debris can originate from the building itself. The debris sources consist of roofing materials such as shingles, tiles, gravel, inadequately attached cladding components such as sheathing and siding, and tree limbs, etc. This chapter further discusses common windborne debris types as a cause of the extreme wind effects on the building envelope.

The components of the building envelope such as windows, doors, curtain walls, and storm shutters play an important role in improving the performance of the building envelope and reducing the damage due to windborne debris. This chapter presents an overview of current test standards to evaluate the performance of the building envelope components against debris impact and also presents the previous research on windborne debris impacts on window glass.

2.1 Common Windborne Debris Types

Minor (1994) analyzed the window damage mechanism during wind storms and classified windborne debris as either small or large missiles. The classification is based on the debris's potential impact elevations on the building envelope. Large missiles can impact the building envelope near ground level, while small missiles can impact high elevations of a building façade. Unanwa and McDonald (2000) classified windborne debris into light-, medium- and heavy-weight missiles, according to their observed damage performance.

Wills et al. (2002) classified windborne debris into three categories based on size and shapes (dimensions): compact objects (3D) such as cubic and spherical roof gravels; sheet objects (2D) such as plywood, corrugated iron, roof tiles and shingles; and rod objects (1D) such as bamboo poles and 2x4 timber. FEMA (2000) also lists the classification of debris types, examples and expected damage as shown in Table 2-1.

The next section presents current test standards for testing the building envelope products against debris impact. The test standards are based on the debris classification given above.

2.2 Windborne Missile Impact Test Standards

2.2.1 History of Windborne Missile Test Standards

Current windborne debris test standards have evolved from experience and research over the past 40 years. In 1974, Tropical Cyclone Tracy struck Darwin, Australia. The post-event report indicated that most of the damage to buildings was caused due to a sudden increase in internal pressure, followed by the failure of windward windows due to windborne debris damage and the fatigue failure of cladding and metal connections under fluctuating pressure (Minor 1994). The first test standard for missile impact appeared shortly thereafter in the Darwin Area Building Manual (Minor 1994). A 4 kg (9 lb) 51mm x 102 mm (2x4) timber appeared as a design missile in the building code. In 1983, a windborne debris impact standard using a 4100 gm (9 lb) 51 mm x 102 mm (2x4) timber as a representative missile was proposed in the Southern Building Code Congress International (SBCCI 1983). The proposal was opposed by major glass manufacturers and was eventually defeated (Hattis 2006). The first building code in the U.S. to incorporate a windborne debris impact standard was the South Florida Building Code (Minor 2005). The standard was adopted in 1993, primarily as a result of the damage caused by Hurricane Andrew (1992) and Hurricane Alicia (1983). The Dade County Building Code Committee initially selected roofing tile as a representative missile, since it was the most prevalent debris in Hurricane Andrew. However, it was observed that it would be difficult to define a representative roofing tile for use in test standards because there were many types of roofing tiles. It was purported that it would be difficult to propel a piece of roofing tile, repeatedly, in the same orientation and at the same speed as a part of a standard test. Ultimately, the committee recommended a 4 kg (9 lb) 51 mm x 102 mm (2x4) timber traveling at 15 m/sec (50 ft/sec) as representative of a large missile in standard tests (Minor 1994). Broward County, Florida, also adopted the windborne debris standard in 1993. These changes were included into Dade County and Broward County editions of the South Florida Building Code (SFBC). Palm Beach County also adopted windborne debris standard in 1994. It was later incorporated into the Standard Building Code (SBC).

2.2.2 American Society of Testing and Materials (ASTM)

ASTM is an international organization that develops technical standards for a wide range of materials, products, and systems using a consensus process. ASTM provides two protocols for testing products for missile impact resistance.

2.2.2.1 The ASTM E 1886-02 (Standard test method for performance of exterior windows, curtain walls, doors and storm shutters impacted by missile(s) and exposed cyclic pressure differentials)

The test standard outlines a method to test products using a missile propulsion device and an air-pressure cycling testing chamber to obtain the conditions similar to debris impact and fluctuating pressures in windstorm events. An air cannon is used to propel small or large missiles to test the products. The test chamber is pressurized with a controllable blower or compressed air supply or vacuum chamber to replicate the effects of static pressure differentials on the test products. The test method evaluates the performance of specimens against the impact of small and large missiles.

The representative small missile is a 2 gm (±5%) steel ball, with an 8 mm nominal diameter, and its impact speed is between 40% and 85% of the basic wind speed. The representative large missile is a No. 2 or better Southern Yellow Pine or Douglas Fir 2x4 with a mass between 2.05 kg ± 0.1kg and 6.8 kg ± 0.1kg. Its length is between 1.2m ± 0.1m and 4.0m ± 0.1m. Its impact speed is between 10% and 55% of the basic wind speed. The specified number of cycles of positive and negative static pressure differential is given in the Table 2-2.

2.2.2.2 The ASTM E 1996-03 (Standard Test Method for performance of exterior windows, curtain walls, doors, and storm shutters impacted by windborne debris in a hurricane)

The test standard evaluates the performance of the exterior windows, curtain walls, doors and storm shutters intended for buildings located in hurricane-prone areas. This standard is similar to ASTM E 1886 but provides additional details about the use of missiles of different weights with varying impact speed. The test products are subjected to missile impacts based on basic wind speed, level of protection, and assembly height. The standard defines four different wind zones based on basic wind speed as given in Table 2-3. It also defines three levels of protection.

- Enhanced protection, for buildings and structures designated as essential facilities includes hospitals, emergency treatment facilities, emergency shelters, power-generating stations, national defense structures, etc.
- Basic protection, for buildings and structures not categorized as enhanced protection and unprotected.
- Unprotected, such as buildings and structures subjected to a low hazard to human life in a windstorm, for example, agricultural facilities, storage facilities, certain temporary facilities, etc.

The missile level, its corresponding missile weight, and impact speed are given in Table 2-4. Products are tested as per Table 2-5. Three test specimens are subjected to large missile impacts and small missile impacts. The specifications for large and small missiles are based on ASTM E 1886. The large missile test requires one impact at product’s center and another at its corner as shown in Figure 2-1. The small missile test consists of a total of 30 steel ball impacts, with 10 steel ball impacts at a time, as shown in Figure 2-2.

The test specimen should resist the large or small missile impacts or both with no tear longer than 130 mm or no opening formed through which a 76 mm diameter solid sphere can freely pass, when evaluated upon completion of missile impacts and test loading for wind zones 1, 2 and 3. For wind zone 4, the test specimen should resist the large or small missile impacts or both without penetration of the inner plane of the infill or shutter assembly as well as the criteria of wind zone 1, 2, and 3.

2.2.3 Florida Building Code (FBC) (TAS 201: Impact Test Procedure)

The Florida Building Code is based on the national model building code and national consensus standards and was developed by the Florida Building Commission. It superseded all local codes in Florida and is effective from 2001 as per Chapter 553, Florida Statues - Building Construction Standards. The structural requirements of the South Florida Building Code were incorporated into special sections of the code for the High Velocity Hurricane Zone (HVHZ) (FBC 2001). The test standard for evaluating the performance of building envelope products under the impact of windborne missiles as per FBC is given below.

The test determines the windborne debris impact resistance of exterior windows, glazing, exterior doors, skylights and storm shutters. Three identical test specimens are repeatedly struck with large or small missiles fired from a missile propulsion device. According to FBC 1626.2.4 the large missile test requires that a solid, nominal 4.1 kg 51 mm x 102 mm (2x4) #2 surface dry Southern Pine lumber be fired at 15.2 m/s (50 fps). The test consists of two impacts – one at the product's center and the other at the corner. The test is applicable for openings less than 9.1m (30 ft) above the ground, according to FBC 1626.2.1. According to FBC 1626.3.4, the small missile test requires that a 2 gm solid steel sphere be fired at 40 m/s (130 fps). It consists of three series of 10 repeated impacts. The first impact series is at the specimen's center, the second occurs at a center of large dimension, and the third occurs at a corner of specimen. The test is applicable to openings higher than 9.1 m (30 ft) above the ground.

If all test specimens have successfully completed TAS 201, they are subjected to cyclic pressure loading as per FBC 1625.4. The test specimen should suffer no resulting failure or distress and should have recovery of 90% over maximum deflection.

2.2.4 American Architectural Manufacturers Association (AAMA)

The American Architectural Manufacturers Association (AAMA) is an industry sponsored organization that has established many of the industry standards that are commonly used today. AAMA has developed two specifications for testing the building components under the impact of windborne debris.

2.2.4.1 The AAMA 506 (Voluntary specifications for hurricane impact and cycle testing of fenestration product)

This specification evaluates the ability of windows, doors, skylights, storefront and curtain walls, and sliding glass doors to withstand the impact and pressure cycling associated with hurricane conditions. The requirements of the test apparatus for large/small missile impacts, test specimens and test procedures address the following standards: ASTM E 1886, ASTM E 1996, AAMA 501, AAMA/WDMA/CSA 101/I.S.2/A-440 and AAMA/NWWDA 101/I.S.2.

2.2.4.2 The AAMA/WDMA/CSA 101/I.S.2/A 440 (Standard specification for windows, doors and unit skylights) Clause 5.3.10 (Impact performance)

For checking the performance of windows, doors and unit skylights when subjected to windborne debris impact in high wind events, the specimens should comply with either ASTM E 1996 or AAMA 506.

2.2.5 American Society of Civil Engineers (ASCE 7-05)

The ASCE 7 standard provides minimum load requirements for the design of buildings and other structures that are subject to building code requirements, including wind effects on structures. ASCE 7-05 defines windborne debris regions as “areas within hurricane prone regions located within 1.61 km (1 mile) of the coastal mean high water line where the basic wind speed is equal to or greater than 49.17 m/s (110 mph) or in Hawaii or areas where the basic wind speed is equal to greater than 53.64 m/s (120 mph).” According to section 6.5.9.3 of ASCE 7-05, glazing in windborne debris regions should be impact-resistant or should be protected with an impact-resistant covering. Either of these should comply with requirements set forth in ASTM E 1886 and ASTM E 1996.

2.2.6 Standard Building Code (SSTD 12-94) (SBCCI Test Standard for Determining Impact Resistance from Windborne Debris)

The Building Officials Association of Palm Beach County, Florida, proposed the SSTD 12-94 standard. This standard evaluated the performance of glazed opening systems and storm shutter systems subjected to impacts of windborne debris and cyclic pressure conditions, as in high-wind events. The specimens are repeatedly struck with small or large missiles fired from a missile propulsion device.

As per the standard, the large missile test is conducted using 2x4 timber specimen. The missile’s weight should be 4.1 kg (9 lb), and its length should be 2.59 m (8.5 ft). The impact speed should be between 15.2 and 15.85 m/s. The test specimen should be impacted once at its center and once at a corner. The small missile test is conducted using 2 gm steel balls. The impact speed should be between 39.62 and 40.23 m/s. The test specimen should receive three series of 10 repeated impacts. The first series should be at the specimen’s center, the second should be at a center of large dimension, and the third should be at a corner of the specimen.

Once the test specimens are subjected to large/small missile impacts, the cyclic pressure loading has to be applied. The specimen should be subjected to the large/small missile impacts and resist the cyclic pressure loading with no crack forming longer than 0.13 m (5”) through which air can pass or with no opening through which a 0.077 m (3”) diameter sphere can pass.

2.2.7 International Building Code (IBC) and International Residential Code (IRC)

The Building Officials Code Administrators International (BOCA), Southern Building Code Congress International (SBCCI) and International Conference of Building Officials (ICBO) combined to create the International Building Code (IBC), which is maintained by the International Code Council (ICC). Section 1609 of the IBC contains wind-load provisions and specifies following the requirements of ASTM E 1886 and ASTM E 1996 for glazing protection in windborne debris regions. It also specifies using a large missile impact test as per ASTM E 1996, if glazed openings are located less than 9.144 m (30 ft) from the ground; it specifies using the small missile impact test as per ASTM E 1886, if glazed openings are located higher than 9.144 m (30 ft).

Section R613.7 of the International Residential Code specifies use of ASTM E 1886, ASTM E 1996 and AAMA 506 for testing exterior windows, doors or other fenestration products if buildings are located in windborne debris regions.

2.2.8 The ICC/NSSA Standard on the Design and Construction of Storm Shelters (Draft)

The scope of this standard is meant for the design and construction of shelters for high-wind events like hurricanes, tornadoes. Storm events produce high winds and flying debris, and so it is important to test components of the shelter envelope against windborne missile impacts. One section of the standard outlines the procedure for conducting impact and pressure testing for components of the shelter envelope. It specifies using ASTM E 1886 for the missile impact test apparatus. The impact missile should be 2x4 lumber. Its weight should be 4.1 kg (9 lb), and its length should be 2.438 m ± 0.102 m (8 ft ± 4 in). Missile impact speed should be 0.4 times the shelter design wind speed for impacting vertical shelter surfaces, and 0.1 times the shelter design wind speed for impacting horizontal shelter surfaces. Windows, other glazed openings, and shutters should be impacted at the specimen's center and also at its corner. No more than two impacts should be made on the test specimen. Any perforation of the tested component of the shelter envelope by the design missile is deemed to constitute a failure.

2.3 Previous Research

The scientific basis of the standards identified in the previous section is addressed in this section. The research most relevant to this study was conducted by Texas Tech University and the NAHB Research Center.

2.3.1 Texas Tech University

Beason (1974) investigated the breakage characteristics of glass specimens when subjected to small missile impacts. He considered two different thicknesses of annealed glass, 2.38 mm (3/32") and 6.35 mm (¼"). Test specimens were subjected to missile impacts of 0.61 gm and 5.55 gm steel balls, which were common representatives of roof gravel debris in wind storm events. Using analysis of variance techniques (ANOVA), it was determined that missile size was a significant factor for the breakage of glass, compared with glass area, glass type, and glass thickness. It was also determined that 6.35 mm (¼") glass was as vulnerable to missile impact damage as 2.38 mm (3/32") glass. Harris (1978) also performed experiments on different thicknesses of glass specimens using 5.55 gm and 28.14 gm missiles, and concluded that missile mass was the most important damage indicator.

Bole (1999) investigated the windborne missile impact on window glass at Texas Tech University. The goal of the project was to determine whether the kinetic energy of the projectile was sufficient to define the outcome of missile impact tests. The project consisted of impacting window glass using common debris impact criteria as per ASTM E 1886 and SSTD 12. Bole (1999) tested 6.35 mm (¼") annealed glass, 6.35 mm (¼") and 4.76 mm (3/16") heat strengthened glass, 6.35 mm (¼”) annealed monolithic glass, and 6.35 mm (½”) tempered monolithic glass using 2x4 timber missiles. According to ASTM E 1886, the large missile test criteria specifies using 4.1 kg (9 lb), 2x4 timber missile with an impact speed of 15.2 m/s (50 fps), which is equivalent to 48.4 kg-m (350 ft-lb) of kinetic energy. Glass specimens were impacted by 2x4 timber missiles of 2.04 kg (4.5 lb), 4.1 kg (9 lb), and 8.16 kg (18 lb) shot from air cannon. The impacts were conducted so that they would produce the same kinetic energy of 350 ft-lb by varying the impact velocity. Bole noted data pertaining to motion of the objects involved in the impact. Bole analyzed the data and calculated the angular velocity of the glazing support frame, kinetic energy before and after impact, and angular momentum. The results of these experiments showed that three different missiles of different mass but the same kinetic energy upon impact produced vastly different results. Bole (1999) concluded that the missile’s kinetic energy upon impact cannot predict the outcome of the impact, and also mentioned that energy loss occurred during a missile impact on window glass.

2.3.2 The NAHB Research Center

The National Association of Home Builders (NAHB) Research Center performed impact testing on glass specimens using field observed and standard missile types to represent windborne debris. The goal of the research was to determine a probabilistic relationship between impact magnitude and glass breakage of typical residential annealed glass using both roof shingle and 2x4 missiles (NAHB 2002). Specimens consisted of 0.61 m (2’) x 0.61 m (2’) and 0.61 m (2’) x 1.22 m (4’) glass panels at 2.38 mm (3/32”) and 3.97 mm (5/32”) thicknesses. All tests were conducted on annealed glass. The study found that a common glazing material provided non-negligible resistance to impacts from 2x4 and roof shingle missiles. It was also observed that when glass specimens were subjected to the impact of roof shingles, the resistance of glass specimens increased proportionally with thickness. The impact resistance of 0.61 m (2’) x 1.22 m (4’) panels was less as compared to that of 0.61 m (2’) X 0.61 m (2’) panels when subjected to shingle missiles. The results also showed that the performance of most glass specimen types was similar for a 2x4 lumber missile.

2.4 Windborne Debris Damage Models

Wills et al. (2002) developed a theoretical model for the UN International Decade for Natural Disaster Reduction. He indicated the damage potential of flying debris is based on the assumption that the amount of damage sustained is proportional to the missile’s kinetic energy. He defined the relationship between the body dimension and the wind speed (V) at which flight occurred and the objects became airborne missiles. The flight speed threshold for compact, sheet and rod objects were, respectively, as follows:

$$V = \sqrt{0.5 * (l * g) * (\frac{\rho_m}{\rho_{air}}) * (\frac{I}{C_f})} \qquad (2\text{-}1)$$

$$V = \sqrt{2 * t * g * (\frac{\rho_m}{\rho_{air}}) * (\frac{I}{C_f})} \qquad (2\text{-}2)$$

$$V = \sqrt{0.5 * (\pi * d) * (\frac{\rho_m}{\rho_{air}}) * (\frac{I}{C_f})} \qquad (2\text{-}3)$$

Where l = characteristic length of compact object, t = thickness of sheet object, d = effective diameter of rod-type object, ρ_m = density of object material, ρ_a = air density, C_f = aerodynamic coefficient, I = fixing strength integrity parameter (for objects resting on the ground I=1), g = gravitational constant. A series of wind-tunnel experiments were conducted at Colorado State University to validate the model for cubes of various material densities and the model for various types of sheet. The damage caused due to a single missile impact can be represented by the kinetic energy equation,

$$D = 1/2 * \rho m * l^3 * V^2 \qquad (2\text{-}4)$$

The equation indicates that damage is directly proportional to the velocity (V) and size of missile. The model indicated that less-dense, compact objects became airborne very easily and had more damage potential at a given wind speed. It was also observed that sheet and rod objects had generally more damage potential than compact objects. (Holmes 2002).

Twisdale et al. (FEMA 2003) developed a windborne debris model to estimate impact risk in residential environments. The model incorporates missile sources and a transport model for the flight of missiles. The model focuses on debris produced from the roofs of residential structures, includes debris as roof tiles, roof shingles, roof sheathing panels, 2x4 lumber, whole roofs, and roof canopies. The model provides information on the total number of impacts to residential building components, impact speed of object, angle and orientation of object when it strikes the building; the model calculates the associated energy and momentum of the missile. The model also calculates the probability of damage to an opening, ($P_V(D)$) for wind speed V,

$$Pv(D) = 1 - \exp[-\lambda * q(1 - P(\xi < \xi d))] \tag{2-5}$$

Where ξd = energy or momentum level assumed to produce damage, q = fraction of building surface occupied by windows and glass doors, λ = mean number of missile impacts per building. The probability of no damage R is given by

$$R = 1 - Pv(D) \tag{2-6}$$

The model generates the probability curves as a function of wind speed, and specifies the probability of exceeding a threshold value of energy or momentum for a window or door.

2.5 Summary

This chapter discusses the causes and types of common windborne debris. Section 2.2 provides information about current test standards for testing building envelope products against missile impact. Section 2.3 presents the past research projects pertinent to our research. Next, chapter 3 discusses the experimental procedure concerning shingle missile impacts on glazing, the apparatus and procedure used during the experiments and results of the experiments.

Table 2-1. Windborne missiles and classification (FEMA 2000)

Missile Size	Common examples of debris	Expected damage
Small (Light Weight)	Aggregate roof surfacing, pieces of trees, pieces of wood framing members, bricks	Broken doors, windows, and other glazing, some light roof covering damage
Medium (Medium Weight)	Appliances, HVAC units, long wood framing members, steel decking, trash containers, furniture	Considerable damage to walls, roof coverings and roof structures
Large (Heavy Weight)	Structural columns, beams, joists, roof trusses, large tanks, automobiles, trees	Damage to wall and roof framing members and structural systems

Table 2-2. Cyclic static air pressure loading (ASTM E1886-02)

Loading Sequence	Loading Direction	Air Pressure Cycles	Number of Air Pressure Cycles
1	Positive	0.2 to 0.5 P_{pos}	3500
2	Positive	0.0 to 0.6 P_{pos}	300
3	Positive	0.5 to 0.8 P_{pos}	600
4	Positive	0.3 to 1.0 P_{pos}	100
5	Negative	0.3 to 1.0 P_{neg}	50
6	Negative	0.5 to 0.8 P_{neg}	1050
7	Negative	0.0 to 0.6 P_{neg}	50
8	Negative	0.2 to 0.5 P_{neg}	3350

Table 2-3. Wind zone classification (ASTM E1996-03)

Wind Zone	Definitions
I	49 m/sec (110 mph) ≤ basic wind speed < 54 m/sec (120 mph) and Hawaii
II	54 m/sec (120 mph) ≤ basic wind speed < 58 m/sec (130 mph) at greater than 1.6 km from the coastline.
III	58 m/sec (130 mph) ≤ basic wind speed ≤ 63 m/sec (140 mph), or 54 m/sec (120 mph) ≤ basic wind speed ≤ 63 m/sec (140 mph) and within 1.6 km of the coastline.
IV	Basic wind speed > 63 m/sec (140 mph)

Table 2-4. Applicable missile (ASTM E1996-03)

Missile Level	Missiles	Impact Speed (m/sec)
A	2 gm ± 5% steel ball	39.62 (130 fps)
B	910 gm ± 100 gm (2.0 lb ± 0.25 lb) 2x4 in	15.25 (50 fps)
C	2050 gm ± 100 gm (4.5 lb ± 0.25 lb) 2x4 in	12.19 (40 fps)
D	4100 gm ± 100 gm (9 lb ± 0.25 lb) 2x4 in	15.25 (50 fps)
E	4100 gm ± 100 gm (9 lb ± 0.25 lb) 2x4 in	24.38 (80 fps)

Table 2-5. Missile impact test for appropriate level of building protection (ASTM E1996-03)

Level of Protection	Enhanced Protection		Basic Protection		Unprotected	
Assembly Height	≤ 9.1 m (30 ft)	>9.1 m (30 ft)	≤ 9.1 m (30 ft)	>9.1 m (30 ft)	≤ 9.1 m (30 ft)	>9.1 m (30 ft)
Wind Zone I	D	D	C	A	None	None
Wind Zone II	D	D	C	A	None	None
Wind Zone III	E	D	D	A	None	None
Wind Zone IV	E	D	D	A	None	None

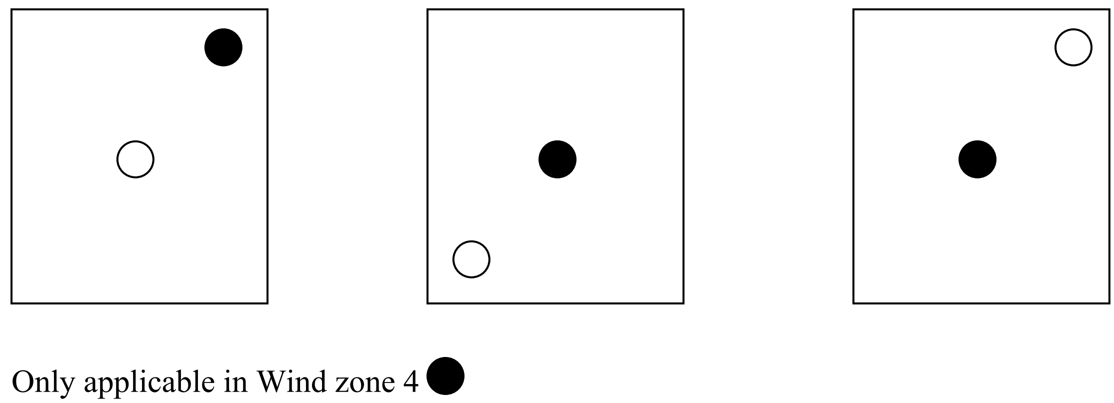

Figure 2-1. Location of large missile impacts on three test specimens (ASTM E1996-03).

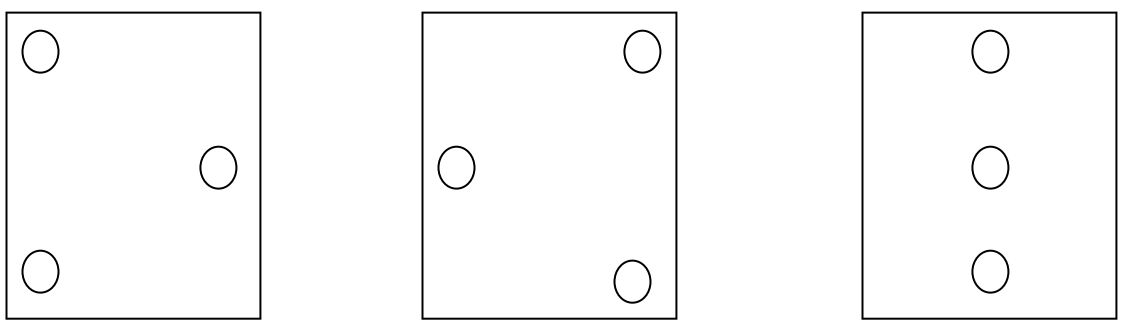

Figure 2-2. Location of small missile impacts on three test specimens (ASTM E1996-03).

CHAPTER 3
IMPACT OF SHINGLE MISSILES ON GLAZING

This first component of the research focuses on the effects of windborne asphalt roof shingles impacting window glass. The study includes an experimental evaluation of the damage threshold of residential glass impacted by roof shingles. This chapter presents the experimental configuration and protocol used in this study and provides the results of the testing.

3.1 Experimental Configuration

In order to simulate windborne asphalt shingle impacts on glazing, an apparatus capable of recreating missile impacts had to be constructed. Its principal components include the shingle launcher, a specimen box and glazing support frame, and a high speed camera. Details of these components are presented in the following sections.

3.1.1 Shingle Launcher

The shingle launcher was designed to propel asphalt shingle missiles of various sizes at various speeds over a short distance into a glass specimen. The design was inspired by a baseball pitching machine. Two vertically oriented rubber tires of 0.19 m (7.5 in) radius contact each other at the treads, and a 0.75 KW (1 hp) Franklin Electric AC induction motor spins the bottom tire, which causes the top tire to contra-rotate (Figure 3-2). The shingle specimens are slowly fed into the gap on a flat plate (tray) into the grip of the spinning tires. The rotation of the tires accelerates the shingle until it is expelled on the opposite side. A motor controller allows the angular velocity of the tires to be adjusted from 250 to 2400 RPM, which in turn determines the velocity of the projectile. The tray can be adjusted to create at least two flight modes: (1) one axis autorotation (Autorotation mode) and (2) tumbling, the latter of which causes the shingle to strike the target on its flat side. The impact location can be changed by rotating and tilting the shingle launcher as required.

3.1.2 Specimen Box and Glazing Support Frame

A 1.42 m (56 in) deep x 1.22 m (48 in) wide x 2.44 m (96 in) tall wood frame box sheathed in 1.27 cm plywood was built to house the glazing support frame and to contain the broken glass for easy disposal. On the side facing the shingle launcher, the specimen box has a 1.03 m (40.5 in) wide x 1.14 m (45 in) high opening through which the shingle passes (Figure 3.1). A glazing support frame holds the glass inside the box. It consists of a fixed wood frame and removable steel frame that supports different sizes and thicknesses of glass. During testing glass specimens are clamped in place between strips of weather-stripping. The frame provides continuous support around the top and bottom of the glass pane.

3.1.3 A High-Speed Camera

A Vision Research Phantom V5.2 high speed camera captured color footage of the shingle missile projectile in flight to determine the projectile velocity. The camera recorded 1000 frames per second after it was configured for 1152 X 896 pixel frame resolution. A 3.05 m (10 ft) long x 0.20 m (8 in) wide board marked with vertical reference at 0.025 m (1 in) intervals was located on the opposite side such that the shingle passed between the board and camera. Reference lines were also marked on the shingle to quantify the angular velocity. Appendix B provides a sample impact velocity calculation.

3.2 Test Materials

The test specimen matrix consisted of annealed glass of varying thicknesses and sizes. All glass specimens were manufactured by Shea's Glass Company located in Gainesville, Florida. Four types of asphalt shingle were used. The new shingles were 3-tab shingles manufactured by Tamko Building Products, which conform to the ASTM D 3462 requirements for asphalt shingles made from glass felt and surfaced with mineral granules. Used shingles were acquired during a re-roofing of a residential home in south Florida. The age of the shingle was estimated to be on the order of 20-30 years. Full-weight and half-weight shingles were used as missiles. To make the half-weight shingles, the full-weight shingles were cut as shown in Appendix D. The test specimen matrix is summarized in Table 3-1.

3.3 Experimental Procedure

3.3.1 Installation of Test Specimen

The first step consists of clamping and securing the glass specimen into glazing support frame. Weather-stripping is used to provide continuous support at top and bottom of the glass pane.

3.3.2 Preparation of Shingle Missile

Each piece of shingle was assigned a unique identification number and its weight was measured.

3.3.3 Missile Impact on Glazing

It was not cost effective to test a new glass specimen for each test. Discarding unbroken specimens would have significantly increased the cost of the experiment. Thus the investigator adopted the following approach.

The shingle was placed on a flat plate (tray) on the shingle launcher. The motor RPM was brought to the required speed and recorded. Next the shingle was slowly fed into the gap between the tires. After impact, the nature of damage (if any) on the glass was also recorded, for example, a crack or shatter. If a break occurred, the next test specimen was mounted and tested at that specified RPM. If a break did not occur, the motor speed was increased by 50 RPM and the test was repeated. This process occurred until the glass broke. Once the glass broke, a new glass specimen was reloaded and the test was repeated until failure. Thus, some conservativeness is built into the procedure, as the specimens usually failed 1-2 iterations after initial impact.

3.3.4 Interpretation

Ideally, slowly increasing the RPM (speed) and using repeat impacting until failure identifies the lowest speed at which that specimen will break from impact of the test shingle. However, this is only the case if damage does not accumulate in the specimen from impacts at lower speeds prior to breakage. The test protocol required that the glass specimen be inspected for visible damage of any kind. Additional impacts at higher speeds were only conducted if no such damage can be identified. Visual inspection is not a foolproof means of determining whether the specimen is damaged.

The purpose of repeating the damage impact speed on a new specimen after the original specimen breaks is to establish whether unseen damage accumulation from multiple impacts on the first specimen could be a factor in its final breakage speed. If damage accumulation is not a factor (the desired circumstance), then subsequent new glass specimens will break at a shingle speed at, or close to, the damage speed of the first sample.

The failure of a second specimen to break at the damage speed of the first specimen in a given test series does not prove that damage accumulation was a factor. Natural variability in glass and shingle specimens, impact location, and other factors will render the damage impact speed a random variable that will be uncertain even with all controllable factors precisely the same. Over the course of many test series, a pattern must emerge where the second specimen usually survives the impact speed of the first specimen in order for damage accumulation to be considered a factor. No such pattern has emerged in the existing dataset. Although the second specimen in several test series does survive the damage speed of the first specimen, in many other test series the second specimen breaks from first impact at the speed of the first specimen that endured multiple incrementally faster impacts.

The breaking speeds of individual glass specimen represent random samples of the minimum-speed-to-damage random variable. However, it is not appropriate to use those specimens that broke at first impact as samples of this variable. That is, the impact test that closes any given test series is not to be used as a minimum-speed-to-damage random sample. Since there was no incremental speed increase on such specimens, they may well have failed at a speed lower than the single impact test speed. The role of these specimens, as defined above, is to provide a means to evaluate the potential influence of damage accumulation in the previous specimens.

3.4 Results

The sample data worksheet is shown in Appendix A. The relationship between the motor RPM and actual shingle speed was calibrated using a high-speed camera. Appendix B shows the calculations for the coefficient of grip. The coefficient of grip relates the tangential speed of the wheels to the shingle coming off the launcher. Appendix C shows the glass breakage velocity with due consideration of coefficient of grip.

Using Equation 3-1, the impact momentum of the shingle was calculated.

$$Momentum = m * v \qquad (3\text{-}1)$$

Where m = mass of shingle, v = velocity of shingle at which glass breaks. Table 3-2 lists the observed momentum values. The kinetic energy of the missile was also calculated using Equation 3-2.

$$KineticEnergy = \tfrac{1}{2} * m * v * v \qquad (3\text{-}2)$$

where m = mass of shingle, v = velocity of shingle at which glass breaks. The values are provided in Table 3-3.

3.5 Discussion of Results

From the data collected from the above experiments, statistical analysis was performed.

Based on ANOVA analysis, following interpretations may be concluded.

- A one-way ANOVA test was performed to determine if the mean momentum required to break the glass varied with glass thickness. As shown in Table 3-4, the F value is very large compared with the critical F value. We can reject the null hypothesis that both groups perform equally. Thus the momentum required to break different thicknesses of glass differs significantly. The mean breakage velocity is 1.47 times higher for 4.76 mm (3/16 in) glass compared with 3.18 mm (1/8 in) glass. As glass thickness increases, the momentum required to break the glass also increases.

- A one-way ANOVA test was performed to determine if the mean momentum required to break the glass varied with the glass size. As shown in Table 3-5, the F value is very small compared with the critical F value. We can accept the null hypothesis that both groups perform equally. The mean threshold momentum is 4.71 kg*m/sec and 4.8 kg*m/sec for 2x2 and 2x4 glass, respectively. Thus, for the range of frontal areas tested, the momentum threshold is not a function of specimen size.

- A one-way ANOVA test was performed to determine if the mean momentum required to break the glass varied with the size and weight of shingle. As shown in Table 3-6 and Table 3-9, the F value is large compared to the critical F value. We can reject the null hypothesis that both groups perform equally. It would also appear that the shingles of different weight do not have same effect for determining momentum to break the glass.

- A one-way ANOVA test was performed to determine if the mean momentum required to break the glass varied with the age of the shingle missile. As shown in Table 3-7 and Table 3-8, the F values are low compared to the critical F values. We can accept the null hypothesis that both groups perform equally. The results indicate that the difference in breakage threshold between new and old shingles is insignificant.

- A one-way ANOVA test was performed to determine if the mean momentum required to break the glass varied with the flight mode of shingle missile. As shown in Table 3-10, the F value is low compared to the critical F value. We can accept the null hypothesis that both groups perform equally. The results indicate that the difference in breakage threshold between Autorotation and Tumbling mode of flight is insignificant.

Conclusions based on the results for the testing are presented in Chapter 5.

Table 3-1. Test specimen matrix

Group	Test specimen	Aspect ratio (hXw)	Number of specimens	Type of shingle	Mode of flight
1	0.61 m (2 ft) x 0.61 m (2 ft) 3.18 mm (1/8 in)	1:1	20	Full weight new shingle	Autorotation
2	0.61 m (2 ft) X 1.22 m (4 ft) 3.18 mm (1/8 in)	2:1	11	Full weight new shingle	Autorotation
3	0.61 m (2 ft) x 0.61 m (2 ft) 3.18 mm (1/8 in)	1:1	20	Half weight new shingle	Autorotation
4	0.61 m (2 ft) x 0.61 m (2 ft) 3.18 mm (1/8 in)	1:1	21	Full weight old shingle	Autorotation
5	0.61 m (2 ft) x 0.61 m (2 ft) 3.18 mm (1/8 in)	1:1	09	Half weight old shingle	Autorotation
6	0.61 m (2 ft) x 0.61 m (2 ft) 4.76 mm (3/16 in)	1:1	12	Full weight new shingle	Autorotation
7	0.61 m (2 ft) x 0.61 m (2 ft) 3.18 mm (1/8 in)	1:1	11	Full weight new shingle	Tumbling

Table 3-2. Threshold momentum for various glass specimens

Momentum (kg*m/sec) (momentum = m*v)						
Mode of flight – Autorotation						Tumbling
3.18 mm (1/8 in) Annealed glass (2x2) Full weight new shingle	3.18 mm (1/8 in) Annealed glass(2x4) Full weight new shingle	3.18 mm (1/8 in) Annealed glass(2x2) Half weight new shingle	3.18 mm (1/8 in) Annealed glass(2x2) Full weight old shingle	3.18 mm (1/8 in) Annealed glass(2x2) Half weight old shingle	4.76 mm (3/16 in) Annealed glass(2x2) Full weight new shingle	3.18 mm (1/8 in) Annealed glass(2x2) Full weight new shingle
2.90	3.59	2.35	3.02	2.48	5.96	3.35
3.59	4.56	2.29	3.14	3.13	6.28	3.90
3.86	4.83	3.06	3.36	3.25	6.52	4.47
4.51	4.83	3.33	4.28	3.44	6.68	4.36
4.51	4.83	3.25	4.89	4.10	6.59	4.81
4.51	5.09	3.63	5.13	4.58	6.59	4.99
4.71	5.54	4.21	5.54	4.66	6.99	
5.15	5.72	4.20	5.20		7.63	
5.54		4.07	6.20		8.27	
5.41		4.70	6.34			
5.72		4.58	6.51			
6.12		4.25	6.42			
		4.43	7.04			
		5.09				
		5.09				

Table 3-3. Threshold kinetic energy for various glass specimens

Kinetic Energy ($kg*m^2/sec^2$)						
Mode of flight – Autorotation						Tumbling
3.18 mm (1/8 in) Annealed glass (2x2) Full weight new shingle	3.18 mm (1/8 in) Annealed glass(2x4) Full weight new shingle	3.18 mm (1/8 in) Annealed glass(2x2) Half weight new shingle	3.18 mm (1/8 in) Annealed glass(2x2) Full weight old shingle	3.18 mm (1/8 in) Annealed glass(2x2) Half weight old shingle	4.76 mm (3/16 in) Annealed glass(2x2) Full weight new shingle	3.18 mm (1/8 in) Annealed glass(2x2) Full weight new shingle
10.50	15.88	13.12	12.15	15.03	45.61	14.04
15.88	25.72	12.81	12.63	23.33	50.54	17.71
18.66	29.16	22.77	14.90	25.71	52.48	24.96
25.40	29.16	26.34	24.13	28.82	56.43	24.34
25.40	29.16	25.71	31.52	42.01	55.72	28.53
25.40	32.76	32.12	35.11	51.24	55.72	29.59
28.43	37.92	41.15	37.92	54.25	61.94	
33.17	41.46	43.06	35.58		73.71	
37.92		43.62	49.89		86.51	
36.98		52.49	53.58			
41.46		51.24	55.01			
46.78		47.49	54.29			
		51.53	65.12			
		61.61				
		61.61				

Table 3-4. ANOVA test between 0.61 m (2 ft) x 0.61 m (2 ft) x 3.18 mm (1/8 in) glass and 0.61 m (2 ft) x 0.61 m (2 ft) x 4.76 mm (3/16 in) glass using full-weight new shingle

Summary Groups	Count	Sum	Average	Variance		
Group 1	12	56.53	4.71	0.89		
Group 6	9	61.51	6.83	0.50		
ANOVA						
Source of variation	SS	df	MS	F	P-value	F critical
Between groups	23.19	1	23.19	31.96	1.89E-05	4.38
Within groups	13.79	19	0.73			
Total	36.98	20				

Table3-5. ANOVA test between 0.61 m (2 ft) x 0.61 m (2 ft) x 3.18 mm (1/8 in) glass and 0.61 m (2 ft) x 1.22 m (4 ft) x 3.18 mm (1/8 in) glass using full-weight new shingle

Summary Groups	Count	Sum	Average	Variance		
Group 1	12	56.53	4.71	0.89		
Group 2	8	38.99	4.87	0.42		
ANOVA						
Source of variation	SS	df	MS	F	P-value	F critical
Between groups	0.13	1	0.13	0.18	0.67	4.41
Within groups	12.71	18	0.70			
Total	12.84	19				

Table 3-6. ANOVA test between full-weight new shingle and half-weight new shingle for 0.61 m (2 ft) x 0.61 m (2 ft) x 3.18 mm (1/8 in) glass

Summary Groups	Count	Sum	Average	Variance		
Group 1	12	56.53	4.71	0.89		
Group 3	15	58.53	3.90	0.79		
ANOVA						
Source of variation	SS	Df	MS	F	P-value	F critical
Between groups	4.36	1	4.36	5.24	0.030	4.24
Within groups	20.83	25	0.83			
Total	25.19	26				

Table 3-7. ANOVA test between full-weight new shingle and full-weight old roof shingle for 0.61 m (2 ft) x 0.61 m (2 ft) x 3.18 mm (1/8 in) glass

Summary Groups	Count	Sum	Average	Variance		
Group 1	12	56.53	4.71	0.89		
Group 4	13	67.07	5.16	1.86		
ANOVA						
Source of variation	SS	df	MS	F	P-value	F critical
Between groups	1.25	1	1.25	0.90	0.35	4.28
Within groups	32.07	23	1.39			
Total	33.32	24				

Table 3-8. ANOVA test between half-weight new shingle and half-weight old roof shingle for 0.61 m (2 ft) x 0.61 m (2 ft) 3.18 mm (1/8 in) glass

Summary						
Groups	Count	Sum	Average	Variance		
Group 3	15	58.53	3.90	0.79		
Group 5	7	25.64	3.66	0.65		
ANOVA						
Source of variation	SS	Df	MS	F	P-value	F critical
Between groups	0.27	1	0.27	0.36	0.55	4.35
Within groups	15	20	0.75			
Total	15.27	21				

Table 3-9. ANOVA test between full-weight old roof shingle and half-weight old roof shingle for 0.61 m (2 ft) x 0.61 m (2 ft) 3.18 mm (1/8 in) glass

Summary						
Groups	Count	Sum	Average	Variance		
Group 4	13	67.07	5.16	1.86		
Group 5	7	25.64	3.66	0.65		
ANOVA						
Source of variation	SS	df	MS	F	P-value	F critical
Between groups	10.18	1	10.19	6.99	0.016	4.41
Within groups	26.24	18	1.46			
Total	36.43	19				

Table 3-10. ANOVA test between Autorotation mode and Tumbling mode of flight for 0.61 m (2 ft) x 0.61 m (2 ft) 3.18 mm (1/8 in) glass impact by new full-weight shingle

Summary						
Groups	Count	Sum	Average	Variance		
Group 1	12	56.53	4.71	1.89		
Group 7	6	25.88	4.31	0.36		
ANOVA						
Source of variation	SS	df	MS	F	P-value	F critical
Between groups	0.63	1	0.63	0.87	0.36	4.49
Within groups	11.58	16	0.72			
Total	12.22	17				

Table 3-11**.** Results summary of mean threshold velocity, momentum, and kinetic energy for glazing testing

Group	1	2	3	4	5	6	7
Annealed glass	0.61 m (2 ft) x 0.61 m (2 ft) x 3.18 mm (1/8 in)	0.61 m (2 ft) x 1.22 m (4 ft) x 3.18 mm (1/8 in)	0.61 m (2 ft) x 0.61 m (2 ft) x 3.18 mm (1/8 in)	0.61 m (2 ft) x 0.61 m (2 ft) x 3.18 mm (1/8 in)	0.61 m (2 ft) x 0.61 m (2 ft) x 3.18 mm (1/8 in)	0.61 m (2 ft) x 0.61 m (2 ft) x 4.76 mm (3/16 in)	0.61 m (2 ft) x 0.61 m (2 ft) x 3.18 mm (1/8 in)
Shingle type	Full weight new	Full weight new	Half weight new	Full weight old	Half weight old	Full weight new	Full weight new
Flight mode				Autorotation			Tumbling
Mean breakage velocity (m/s)	11.81	12.17	19.13	13.50	17.97	17.35	10.59
Mean momentum (kg*m/s)	4.71	4.8	3.90	5.15	3.66	6.83	4.31
Mean kinetic energy ($kg*m^2/sec^2$)	28.83	30.15	39.11	37.06	34.34	59.85	23.20

A B


Figure 3-1**.** Testing facility. A) Wooden box. B) Glazing support frame.

Figure 3-2. Shingle missile launcher. A) Full view of launcher. B), C), D) Different units of launcher.

A B C D

Figure 3-3 Common glass breakage patterns A) 2x2 1/8” annealed glass (700 RPM). B) 2x2 1/8” annealed glass (800 RPM). C) 2x2 1/8” annealed glass (450 RPM). D) 2x4 1/8” annealed glass (900 RPM). E) 2x4 1/8” annealed glass (750 RPM).

E 

Figure 3.3 Continued.

CHAPTER 4
IMPACT OF ROOFING TILES AND 2X4 MISSILES ON WINDOW SHUTTERS

The second objective of the research concerned the damage caused by tile missile impact on shutters. This chapter presents the experimental configuration and protocol used in this study and provides details on apparatuses used. Results of this testing are presented herein, and are compared to identical tests performed as per the standard large missile (2x4) impact test prescribed in FBC 1626.2.

4.1 Experimental Configuration

To simulate the effect of roofing tiles impacting window shutters, a custom projectile launcher and reaction frame were constructed, and a high-speed camera was used to estimate the velocity of the projectile. This section elaborates on these apparatuses and the experimental procedure.

4.1.1 Reaction Frame and Shutter Mounts

A 1.91 m (75 in) wide x 1.52 m (60 in) tall reaction frame was used to support the shutter assembly (Figure 4-1). The frame was constructed using 4x4 wood members. The reaction frame can accommodate 1.45 m (57 in) high window shutters. The base of the reaction frame was attached to a concrete strong floor using anchor bolts to prevent the frame from sliding upon impact. The shutter systems were installed on the reaction frame using commonly used bottom track and top track at the sill and head of the frame, respectively. A 5.08 cm (2 in) x 5.08 cm (2 in) studded angle served as the bottom track. The shutters were secured into the studded angle sill track using wing nuts. Two styles of shutter mountings were employed in this study: The direct mount method and tracking method. For the direct mount method, shutters were secured directly using 6.35 mm (1/4 in) diameter anchors at the head level. In the tracking method, an H-track was used at the top. Shutters could simply slip up into a header channel without any fasteners.

4.1.2 Tile Projectile Launcher

In this study, a pneumatic ram accelerated the tile missiles to achieve a prescribed flight velocity prior to impact on the test specimen. The ram is powered by air stored in a 75.7 liter (20-gallon) 6.9 kN/m^2 (130 psi) capacity accumulation tank, and a solenoid-operated Magnetrol 10.16 cm (4 in) ball valve connects the tank to the ram. The acceleration of the ram is dependent on the size and speed of the valve, which determines the discharge rate. Accordingly, the valve was selected to achieve a maximum final velocity of 30.48 m/s (100 fps). The valve was operated by 5 V (TTL) signal supplied from a National Instrument USB-6211 module, driving solid state relay to provide the necessary AC power. Pressure in the accumulation tank is monitored using an Omegadyne PX309-150G5B pressure transducer, which is capable of measuring 0 – 1 MPa (0- 150 psi).

The pneumatic ram connects to a 100 mm (4 in) schedule 80 PVC tube. The PVC tube is 1.35 m (4.5 ft) long. Inside the tube, a Delrin plastic disc is attached to an aluminum push rod guided by a hole in the end of the PVC tube (Figure 4-2). A plate is connected to the other end of the push rod, which protrudes from the PVC tube. Two 8020 modular aluminum channels extend from the end of the PVC tube to the full extent of the push rod, and they support a plywood tray covered with a 0.635 mm DuPont Delrin thermoplastic polymer sheet.

The air ram is designed to accommodate a wide range of projectiles. For the tile specimens, it was necessary to adhere 2700 mm x 230 mm x 0.635 mm Delrin pads on the bottom of the tile to ensure that the tile could slide smoothly on the surface.

Multiple safety measures were implemented. Laser diodes ensure the piston that the piston is fully engaged before the tank can be charged. A separate purge valve was incorporated in the design to prevent overcharging the tank. A mechanical overpressure safety valve is also attached to the air tank to prevent over-pressurization of the system.

A custom National Instruments Labview 8.5 program coordinated data acquisition and control system (Figure 4-3). A National Instrument Model monitored the system pressure in the accumulation tank and controlled the valves.

4.1.3 The 2x4 Projectile Launcher

The large missile air cannon used compressed air to launch 2x4 large missiles onto window shutters. A large missile cannon consists mainly of the following components: an air compressor, pressure-release valve, pressure gauge, and a barrel and its support frame.

A 6.1 m (20 ft) barrel rests on an aluminum beam hanging from steel cables supported by a steel tube frame. The barrel height can be adjusted using a pair of winches. One compressor provides the air pressure required to facilitate the launch of the 2x4 missile. A smaller compressor powers the trigger-release mechanism. Once the desired launching pressure is attained, pushing the trigger activates the piston, which opens the release valve. The stopping bolt is located near the firing controls. The stop assures that each missile will be fired from a consistent distance.

4.1.4 A High-Speed Camera

A Vision Research Phantom V5.2 high-speed camera captured color footage of the tile missile projectile in flight to determine the projectile velocity. The camera recorded 1000 fps after it was configured for 1152 x 896 pixel frame resolution. The camera was positioned 1.02 m to the side of the path of the projectile to record a profile view. A 3.05 m (10 ft) long x 0.20 m (8 in) wide board marked with vertical reference lines at 0.025 m (1 in) intervals was located on the opposite side such that the tile passed between the board and the camera. Reference lines were also marked on tiles to quantify the angular velocity. Appendix G provides a sample impact velocity calculation.

4.2 Test Materials

Window shutters were tested using two different missiles. The first missile was concrete tile. The second was a 4.1 kg 2x4 as specified in FBC 1626.2. Galvanized steel storm panels with a thickness of 0.76 mm (0.030 in) were used for testing. Shutters were secured using 6.35 mm (1/4 in) 20 threaded wing nuts on the standard 5.08 cm (2 in) x 5.08 cm (2 in) studded angle at the sill. An H-box was used to secure the top of the shutter (Figure 4.5). It has a 5.08 cm (2 in) wide gap to accommodate the shutter at the top without mounting hardware. Tapcon storm guard anchors of 6.35 mm (¼ in) x 57.15 mm (2¼ in) were used for directly mounting the shutters.

4.3 Experimental Procedure

4.3.1 Installation of Test Specimen Assembly

The first step consisted of installing the bottom track and top track at the sill and head of the reaction frame for the shutters. The studded angle was used as a bottom track, and is an L-shaped angle with a stud member. For the top track, two types of installation methods were used. The first design consisted of sliding shutters into a 5.08 cm (2 in) wide gap of H-track without any mounting hardware including the midspan through bolts at the seams, and the second design consisted of mounting shutters on the reaction frame directly with 6.35 mm (1/4 in) diameter Tapcon SG Anchors at the header. Then storm panels were installed in such a way that panels would overlap each other at the ends. The storm panels were secured into the studded angle at sill level using 6.35 mm (1/4 in) diameter wing nuts.

4.3.2 Preparation of Missiles

Each tile and 2x4 lumber missile were assigned a unique identification number, and their weight was measured and recorded.

4.3.3 Missile Impact on Hurricane Shutters

After the storm panels were mounted on the reaction frame, the missile firing sequence was initiated. Once the test specimen was impacted, the pressure in the tank was purged. The same procedure was repeated for each test specimen. Window shutters were impacted by tile missiles at approximately 15.2 m/s (34 mph) and 20.12 m/s (45 mph). For comparison, window shutters were also impacted by 2x4 lumber missiles at approximately 15.2 m/s (34 mph) and 20.12 m/s (45 mph).

4.3.4 Data Collection

The test date, missile number, type of missile, coordinates of the point of impact, deflection, any penetration or opening, and installation type for shutter were recorded for each test. The sample data worksheet is shown in Appendix E.

4.4 Results

The test plan was designed primarily to simulate actual conditions that common window storm panel systems could experience in a building when subjected to windborne debris impact during extreme winds. All window shutter systems were tested and results are given in Table 4-1 and Table 4-2. The momentum was calculated using Equation 4-1.

$$momentum = m * v \qquad (4\text{-}1)$$

Where m = mass of shingle and v = velocity of the tile

Using Equation 4-2, the kinetic energy was calculated.

$$KineticEnergy = \tfrac{1}{2} * m * v^2 \qquad (4\text{-}2)$$

For each test specimens the values of momentum and kinetic energy are shown in Table 4-3 and Table 4-4.

4.5 Discussion of Results

The results are summarized below:

- Table 4-5 shows the mean deflection values for the shutters when tested at approximately 15.2 m/s (34 mph). The mean deflection of the shutters is 1.45 times higher for a tile missile as compared with a 2x4 missile, when shutters were secured in the H-box at the head.

- Table 4-5 shows the mean deflection values for the shutters when tested at approximately 15.2 m/s (34 mph). The mean deflection of the shutters is 1.2 times higher for a tile missile compared with a 2x4 missile, when shutters were secured using direct anchor at the head. The momentum of the tiles was larger than the 2x4s, which may partially account for this difference.

- An ANOVA test was performed to understand the relationship between the tile missile and 2x4 missile impact for the H-box assembly. Table 4-6 shows that the F value is small compared to the critical F value, therefore we can accept the null hypothesis. The results indicate that the difference in deflection between the impact of a tile missile and a 2x4 missile for the H-box assembly is insignificant.

- An ANOVA test was performed to understand the relationship between the tile missile and 2x4 missile impact for the direct mount assembly. Table 4-7 shows that the F value is small compared to the critical F value, therefore we can accept the null hypothesis. The results indicate that the difference in deflection between the impact of a tile missile and a 2x4 missile for the direct mount assembly is insignificant.

Some additional observations based on the experiments are as follows:

- The shutters were tested at 15.2 m/s (34 mph) under tile missile impact and 2x4 missile impact, for H-box assembly. Shutters can protrude outward at the header under tile missile impact, which makes them vulnerable to becoming windborne debris. (Figure 4-15 and Figure 4-17).

- Shutter testing results show that the performance of the shutters at the header is comparatively better when shutters were directly mounted to the reaction frame rather than using the H-box without any mounting accessories under the impact of tile missile and 2x4 lumber. (Figure 4-15 and Figure 4-20).

Table 4-1. Missile impact test results for round 1 testing at approximately 20.12 m/s (45 mph)

Test	Missile type	Missile speed (m/sec)	Installation type	Damage description	Deflection (m)	Figure
A	Tile	20.550	H-Box	Impact point near the center of shutter	0.216	4.6
		20.552	H-Box	Impact point at seam of shutter	0.191	4.7
B	2x4 lumber	20.117	H-Box	Impact point at seam of shutter, hole size 2.54 cm (1”)	0.162	4.8
		20.117	H-Box	Impact point near the center of shutter, hole size 2.54 cm (1”)	0.187	4.9
		20.117	H-Box	Impact point at seam of shutter, hole size 7.62 cm (3”)	0.194	4.10
C	Tile	19.617	Direct mount	Impact point near the center of shutter	0.146	4.11
		20.550	Direct mount	Impact point at seam of shutter	0.098	4.12
D	2x4 lumber	20.117	Direct mount	Impact point at seam of shutter	0.156	4.13
		20.117	Direct mount	Impact point near the center of shutter, hole size 3.81 cm (1.5”)	0.171	4.14

Table 4-2. Missile impact test results for round 2 testing at approximately 15.2 m/s (34 mph)

Test	Missile type	Missile speed (m/sec)	Installation type	Damage description	Deflection	Figure
E	Tile	16.599	H-Box	Impact point near the center of shutter	0.140	4.15
		15.984	H-Box	Impact point at seam of shutter, hole size 1.91 cm (0.75”)	0.178	4.16
F	2x4 lumber	12.944	H-Box	Impact point near the center of shutter	0.102	4.17
		15.199	H-Box	Impact point at seam of shutter	0.121	4.18
G	Tile	16.599	Direct mount	Impact point at seam of shutter	0.203	4.19
		16.599	Direct mount	Impact point near the center of shutter	0.149	4.20
H	2x4 lumber	15.199	Direct mount	Impact point near the center of shutter	0.165	4.21
		15.199	Direct mount	Impact point at seam of shutter	0.124	4.22

Table 4-3. Momentum and kinetic energy for various test specimens at approximately 20.12 m/s (45 mph)

Test	Missile mass (kg)	Tile speed (m/sec)	Momentum (Kg.m/sec)	Kinetic energy (Joule)(J)
A	4.140	20.550	85.077	874.166
	4.615	20.552	94.847	974.653
B	3.946	20.117	79.382	798.461
	4.350	20.117	87.509	880.209
	4.350	20.117	87.509	880.209
C	4.575	19.617	89.748	880.291
	4.235	20.550	87.029	894.226
D	4.350	20.117	87.509	880.209
	4.350	20.117	87.509	880.209

Table 4-4. Momentum and kinetic energy for various test specimens at approximately 15.2 m/s (34 mph)

Test	Missile mass (kg)	Tile speed (m/sec)	Momentum (Kg.m/sec)	Kinetic energy (Joule)(J)
E	4.460	16.599	74.032	614.425
	4.515	15.984	72.168	576.765
F	4.350	12.964	56.393	365.542
	4.350	15.199	66.116	502.446
G	4.060	16.599	67.392	559.319
	4.215	16.599	69.965	580.673
H	4.350	15.199	66.116	502.446
	4.350	15.199	66.116	502.446

Table 4-5. Results summary of mean threshold velocity, momentum, kinetic energy and deflection for window shutters testing

Window shutters	Tile missile (H-Box)	Tile missile (Direct mount)	2X4 missile (H-Box)	2X4 missile (Direct mount)
Mean speed (m/s)	16.3	16.6	14.1	15.2
Mean momentum (kg*m/s)	73.1	68.7	61.3	66.1
Mean kinetic energy (J)	595.6	570.0	434.0	502.5
Mean deflection (m)	0.16	0.18	0.11	0.15

Table 4-6. ANOVA test between tile missile and 2x4 missile using an H-box assembly at 15.2 m/s (34 mph)

Summary						
Groups	Count	Sum	Average	Variance		
Tile	2	0.318	0.159	0.000722		
2x4	2	0.223	0.1115	0.00018		
ANOVA						
Source of variation	SS	df	MS	F	P-value	F critical
Between groups	0.00225625	1	0.00225625	5	0.154845745	18.51282051
Within groups	0.0009025	2	0.00045125			
Total	0.00315875	3				

Table 4-7. ANOVA test between tile missile and 2x4 missile using the direct mount assembly at 15.2 m/s (34 mph)

Summary						
Groups	Count	Sum	Average	Variance		
Tile	2	0.352	0.176	0.001458		
2x4	2	0.289	0.1445	0.0008405		
ANOVA						
Source of variation	SS	df	MS	F	P-value	F critical
Between groups	0.00099225	1	0.00099225	0.863389167	0.450885251	18.51282051
Within groups	0.0022985	2	0.00114925			
Total	0.00329075	3				

Figure 4-1. Reaction frame.

A

Figure 4-2. Tile missile launcher. A) Full view. B) View of different units of launcher.

B

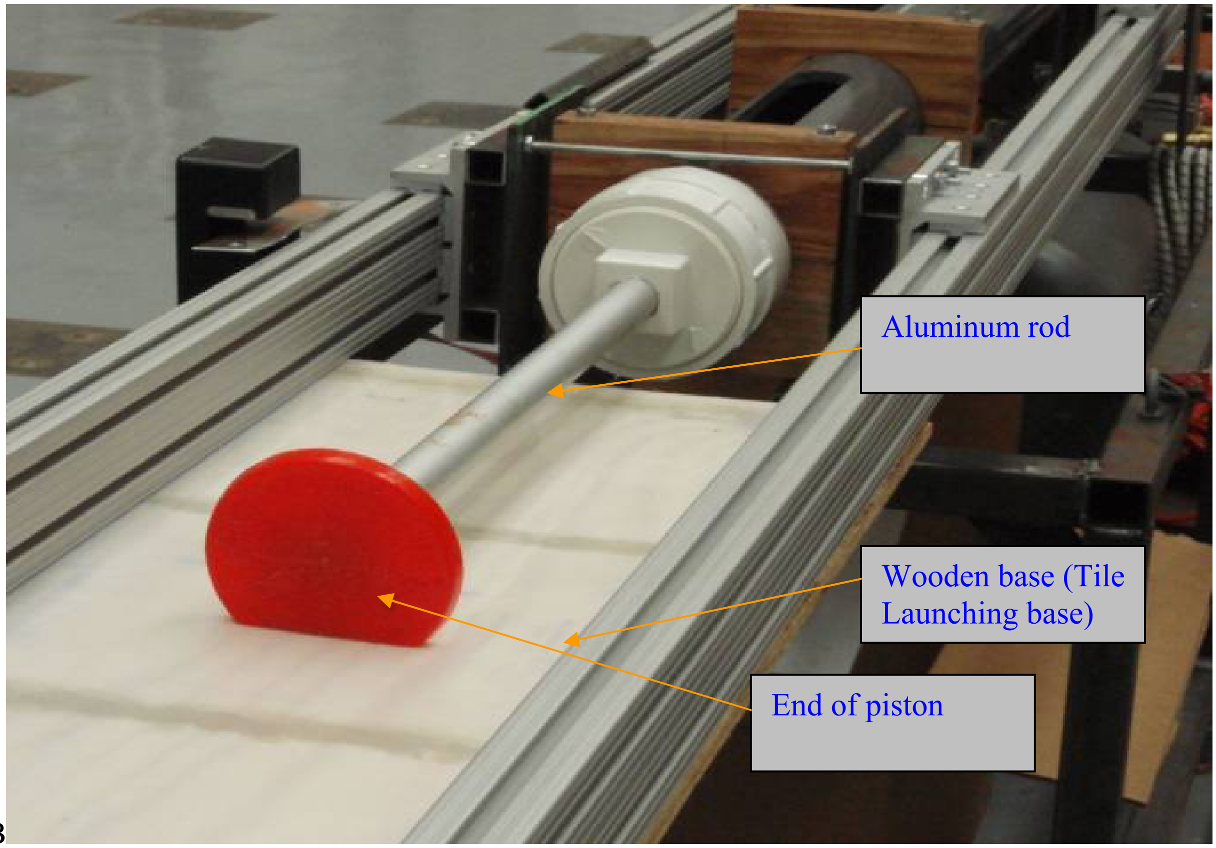

Figure 4-2. Continued

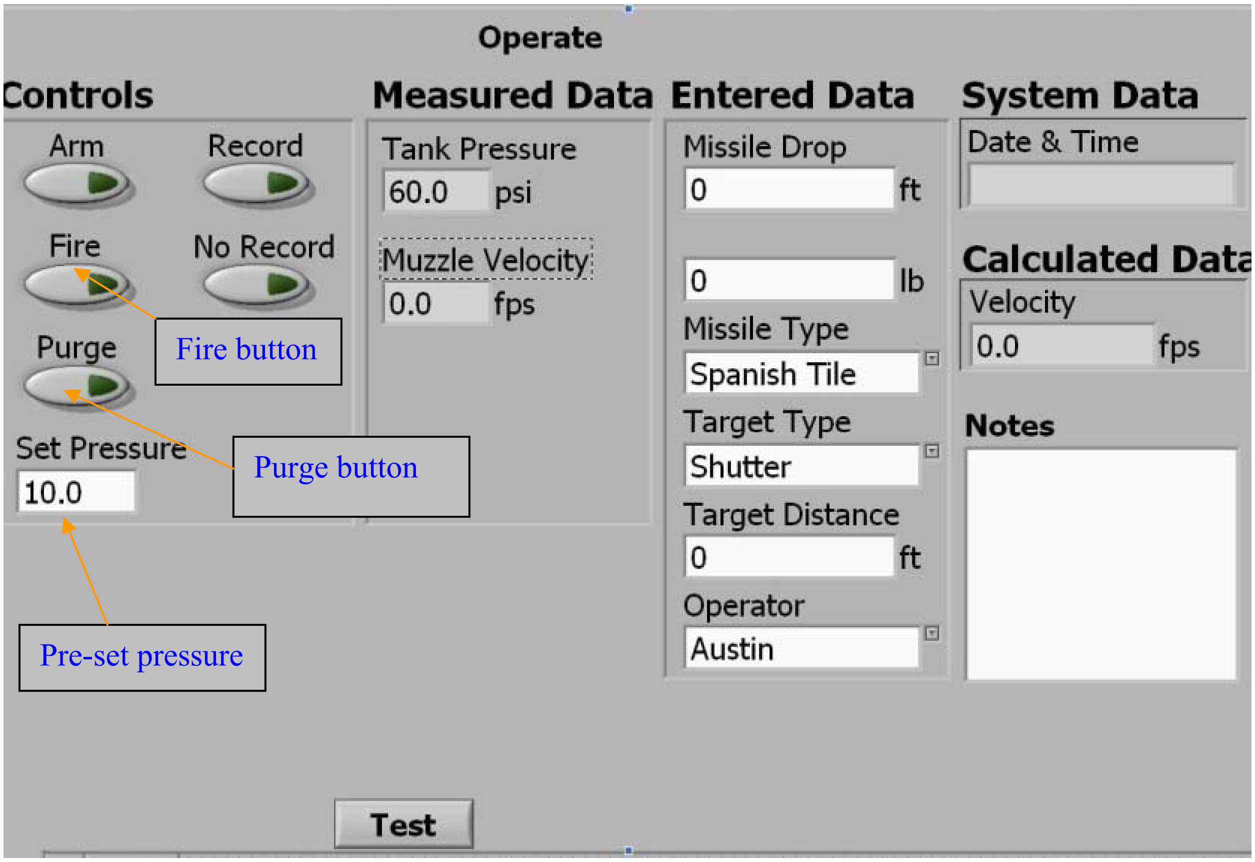

Figure 4-3. Labview program view for tile missile launcher

Figure 4-4. Board marked with reference lines spaced at 2.54 cm (1 in)

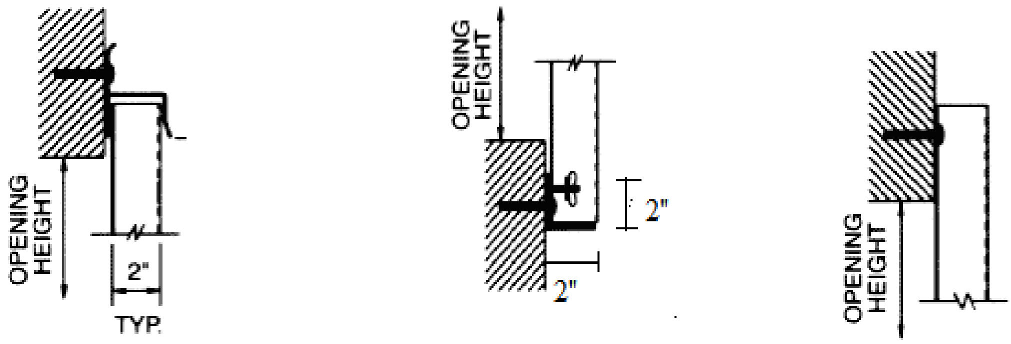

A B C

Figure 4-5. Types of installation at header and sill level. A) Standard “H” header. B) Stud angle at bottom track. C) Direct mount at header.

Figure 4-6. Tile missile impact test for H-box assembly, center shot (Test A-1)

Figure 4-7. Tile missile impact test for H-box assembly, seam shot (Test A-2)

Figure 4-8. 2X4 lumber missile impact test for H-box assembly, seam shot (Test B-1)

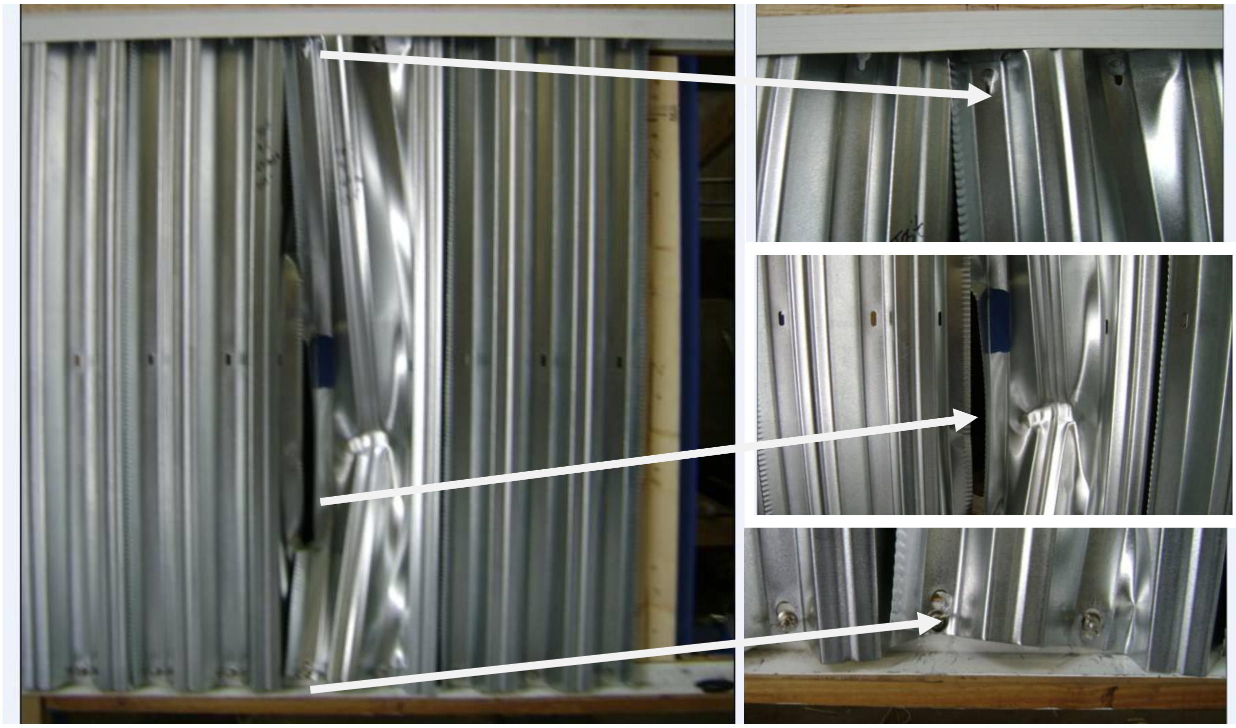

Figure 4-9. 2X4 lumber missile impact test for H-box assembly, center shot (Test B-2)

Figure 4-10. 2X4 lumber missile impact test for H-box assembly, seam shot (Test B-3)

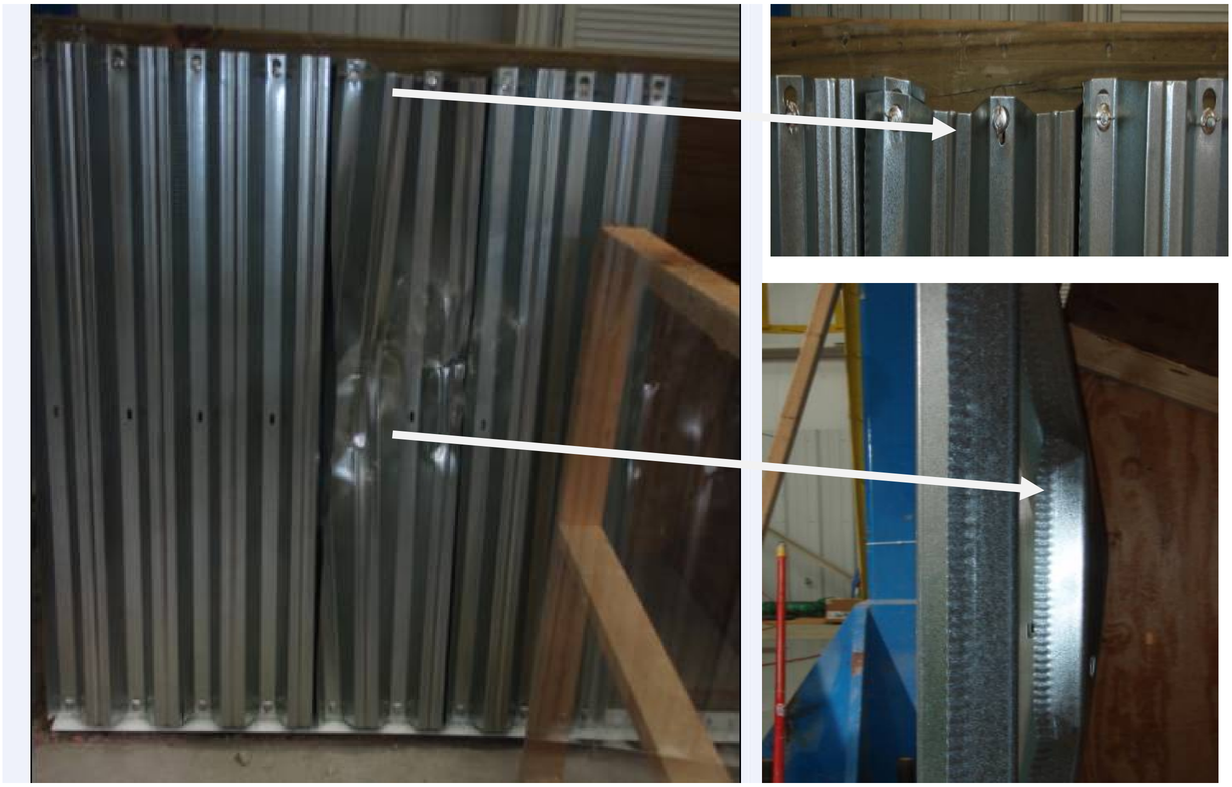

Figure 4-11. Tile missile impact test for direct mount assembly, center shot (Test C-1)

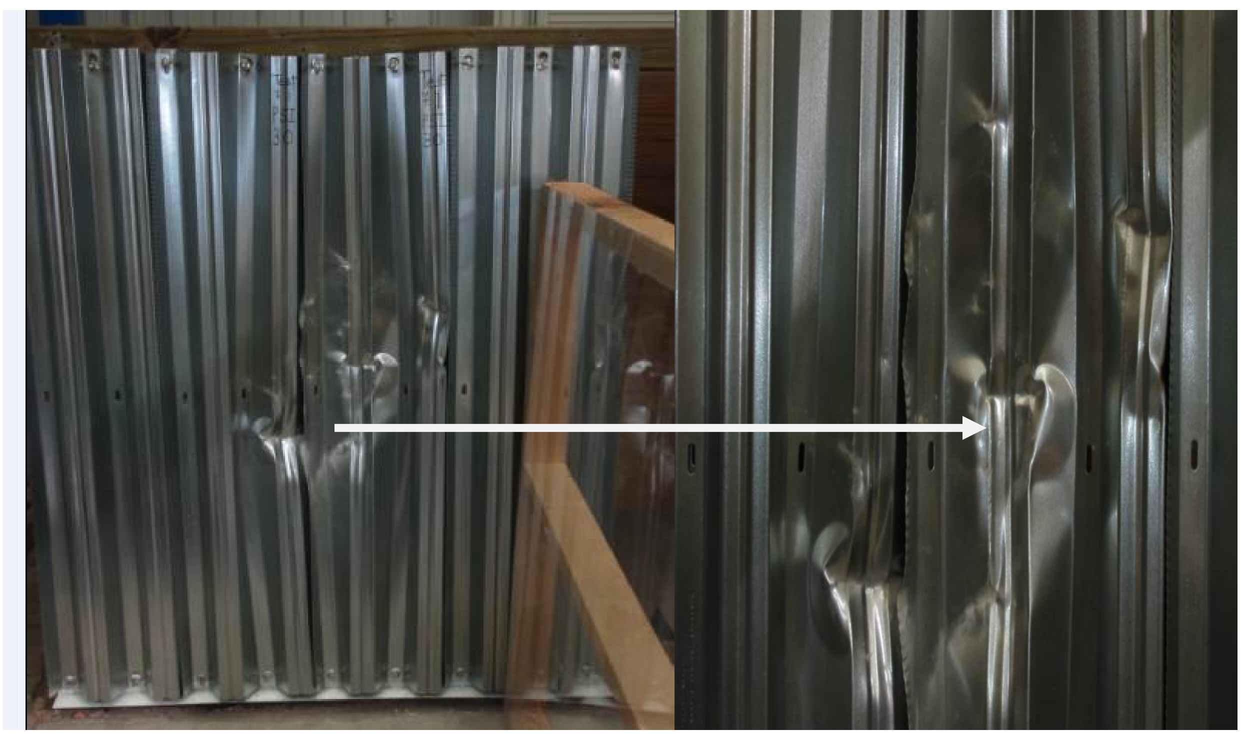

Figure 4-12. Tile missile impact test for direct mount assembly, seam shot (Test C-2)

Figure 4-13. 2X4 lumber missile impact test for direct mount assembly, seam shot (Test D-1)

Figure 4-14. 2X4 lumber missile impact test for direct mount assembly, center shot (Test D-2)

Figure 4-15. Tile missile impact test for H-box assembly, center shot (Test E-1)

Figure 4-16. Tile missile impact test for H-box assembly, seam shot (Test E-2)

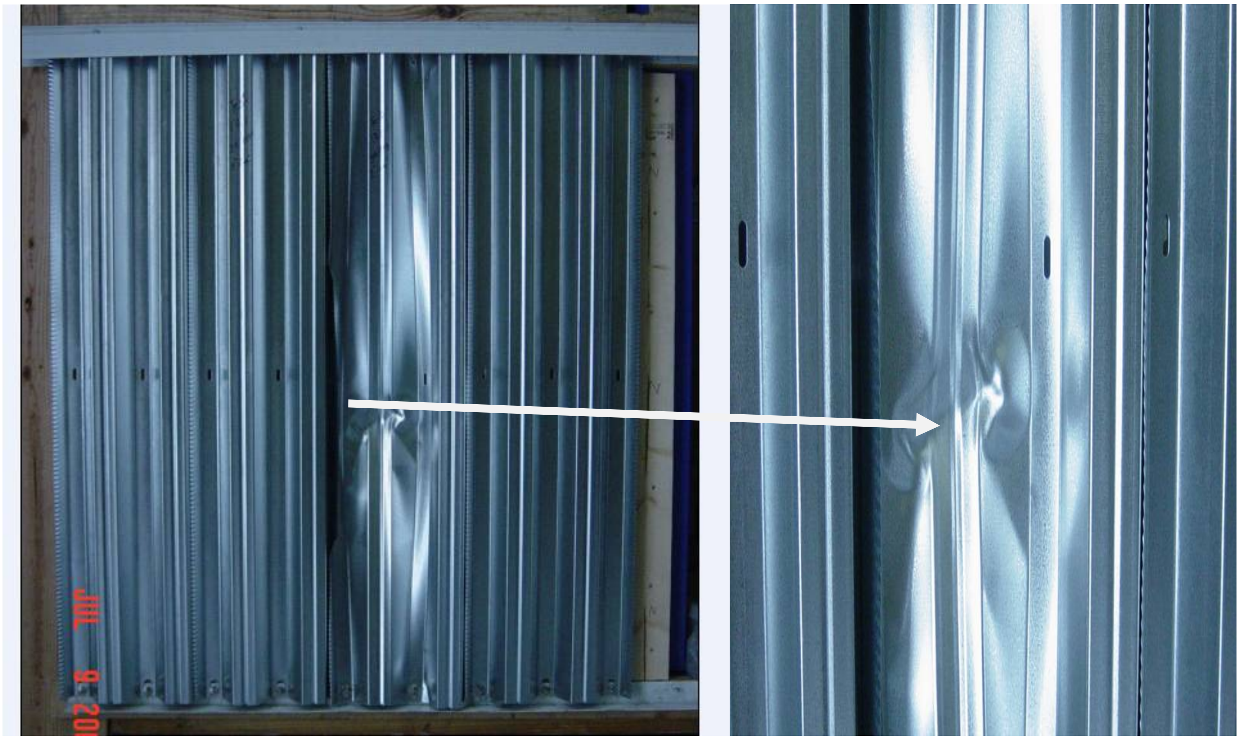

Figure 4-17. 2X4 lumber missile impact test for H-box assembly, center shot (Test F-1)

Figure 4-18. 2X4 lumber missile impact test for H-box assembly, seam shot (Test F-2)

Figure 4-19. Tile missile impact test for direct mount assembly, seam shot (Test G-1)

Figure 4-20. Tile missile impact test for direct mount assembly, center shot (Test G-2)

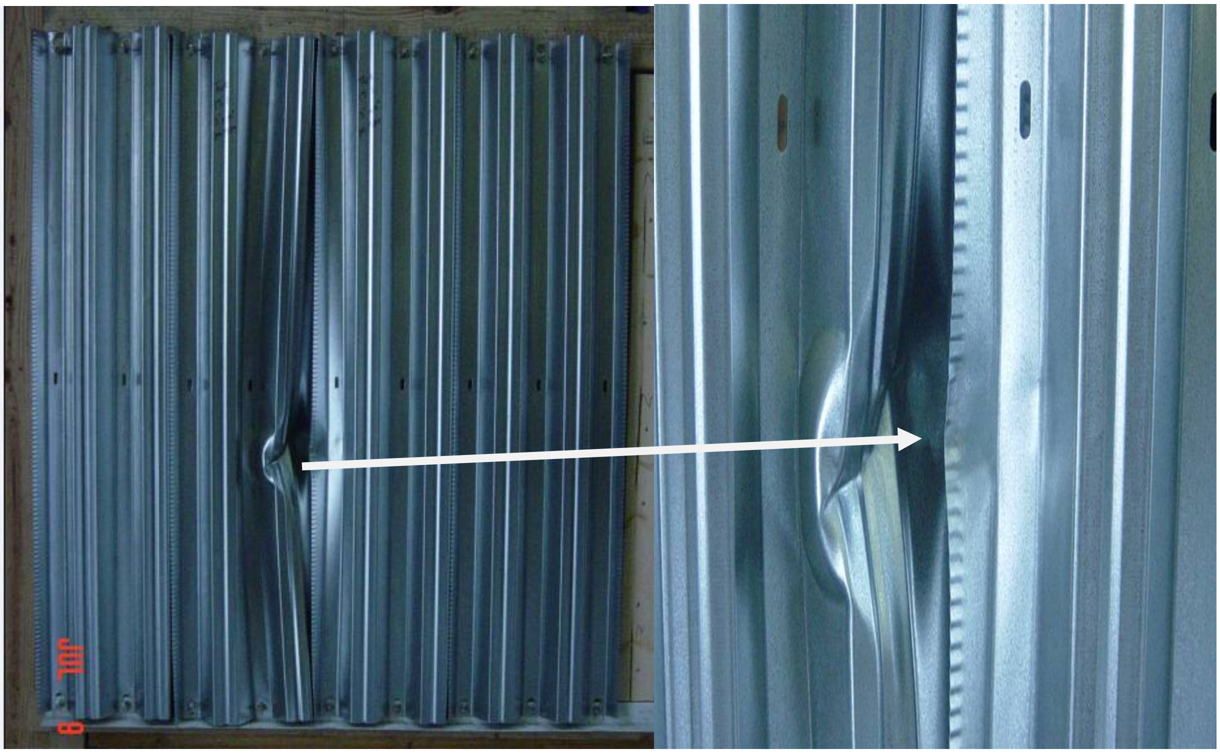

Figure 4-21. 2X4 lumber missile impact test for direct mount assembly, center shot (Test H-1)

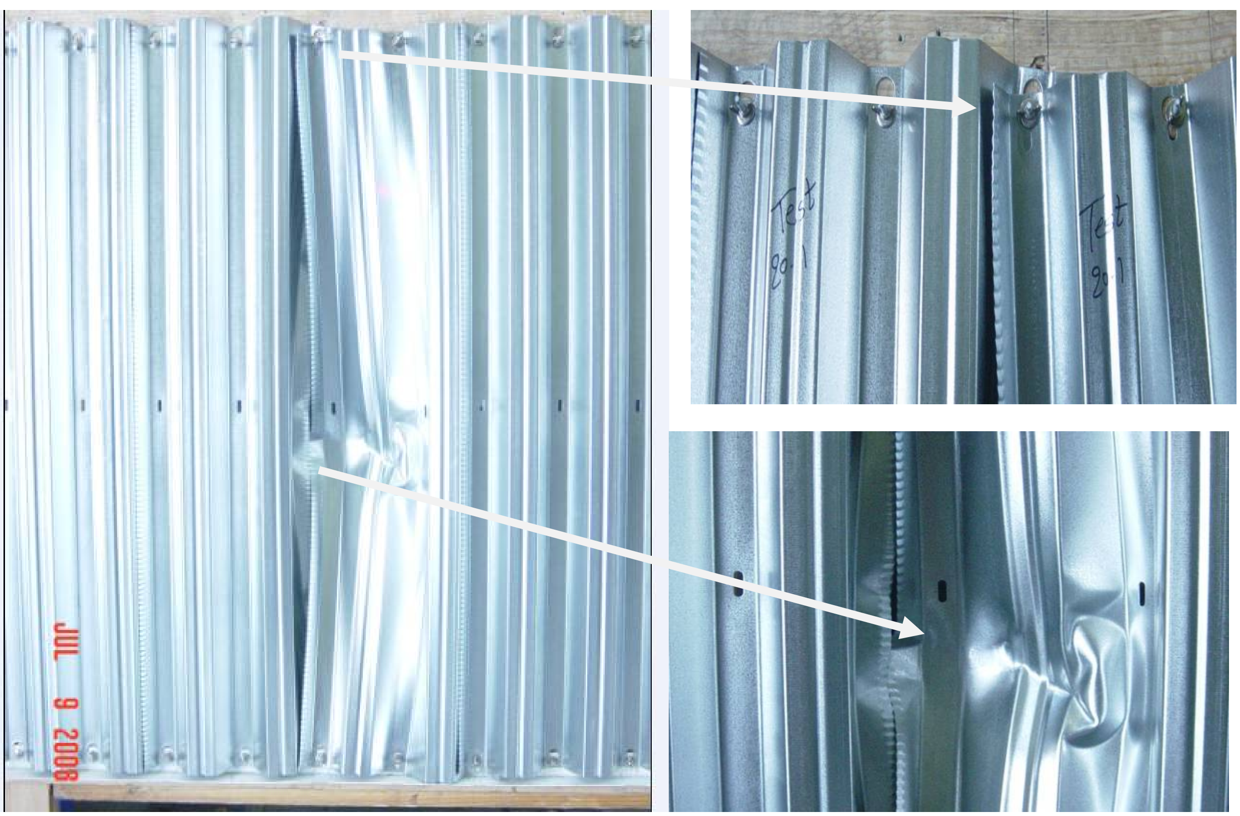

Figure 4-22. 2X4 lumber missile impact test for direct mount assembly, seam shot (Test H-2)

CHAPTER 5
CONCLUSIONS AND RECOMMENDATIONS

5.1 Conclusions

Based on the findings in Chapters 3 and 4, this chapter presents conclusions and recommendations regarding the impacts of shingle missiles on glazing and tile missiles on window shutters.

5.1.1 Impact of Shingle Missiles on Glazing

Window glazings of varying thickness and span were subjected to simulated windborne shingle impacts in order to provide a statistical quantification of the threshold of damage. Both new and naturally aged shingles were used for testing the glazing. The conclusions from this research are as follows:

- Two different glass thicknesses were considered for testing. As glass thickness increases, the momentum required to break the glass also increases. The mean breakage velocity of 4.76 mm (3/16") glass is 1.47 times greater than 3.18 mm (1/8") glass.

- The mean breakage velocity for Group 1 (2x2 glass – full-weight new shingle) and Group 2 (2x4 glass – full-weight new shingle) is approximately 12 m/sec. The mean threshold momentum for both size of glass is 4.71 kg*m/sec and 4.8 kg*m/sec, respectively. Based on an ANOVA test, it was found that there was no statistically relevant difference in speed and momentum when comparing 0.61 m (2') x 1.22 m (4') to 0.61 m (2') x 0.61 m (2') 3.18 mm (1/8") glass specimens. It indicates that the momentum threshold is not a function of specimen size for the range of frontal areas tested.

- For the roof shingle missile, the impact momentum causing a breakage ranged from 2.35 to 7.04 kg*m/sec for the 3.18 mm (1/8") annealed glass specimens.

- For the roof shingle missile, the impact momentum causing a breakage ranged from 5.96 to 8.27 kg*m/sec for the 4.76 mm (3/16") annealed glass specimens.

- Full-weight shingles required a mean threshold momentum of 4.71 kg*m/s and 5.15 kg*m/s for new and old shingles, respectively. Half-weight shingles required a mean threshold momentum of 3.90 kg*m/s and 3.66 kg*m/s for new and old shingles, respectively. Based on mean momentum values and ANOVA analysis, these results indicates that new or old shingles perform equally well in breaking the glass window, but different weight shingles do not have the same effect on the glass.

- For the roof shingle missile, the kinetic energy causing breakage ranged from 10 kg*m/sec to 65 kg*m/sec for 3.18 mm (1/8”) annealed glass.

- For the roof shingle missile, the kinetic energy causing breakage ranged from 45 kg*m/s to 86 kg*m/sec for 4.76 mm (3/16”) annealed glass.

- Momentum appears to be the appropriate benchmark parameter when determining likelihood of glass breakage.

- Glass specimens of 0.61 m (2 ft) x 0.61 m (2 ft) x 3.18 mm (1/8 in) were tested under Tumbling flight mode with a new full-weight shingle. The mean threshold momentum for Tumbling mode is 4.31 kg*m/s and for Autorotation mode is 4.71 kg*m/s.

5.1.2 Impact of Roofing Tiles and 2x4 Missiles on Window Shutters

This research project was conducted to determine information concerning the behavior of commonly used storm panels under large missile impact, using roofing tiles and 2x4 lumber. The following conclusions were drawn from the examination of tested hurricane storm panels and the results obtained from the collected data.

- The mean deflection of the shutters is 1.45 times higher for tile missile compared with the 2x4 missile, when shutters were secured in the H-box at the head.

- The mean deflection of the shutters is 1.2 times higher for the tile missile compared with the 2x4 missile, when shutters were secured using the direct anchor at the header.

- The results clearly showed that directly mounted panels performed well compared with the H-box assembly at the header of the shutter. The shutters protrude outward at the header when impacted using a tile missile for H-box assembly at 15.2 m/s (34 mph). (Figure 4-15, 4-17, 4-20).

5.2 Recommendations for Future Research

The results of the study about window glazing behavior against impact of shingle missile should be used to improve risk modeling of windborne debris and to improve glazing performance.

- In the experimental setup, the glazing was supported on two sides only. Additional testing should be conducted with the glazing supported along its entire perimeter.

- Additional testing should be conducted on double-pane glass.

- In the experimental setup, the glazing was tested against missile impact. Actual windows should be tested further in order to see the behavior of actual windows against shingle missile impact. From the window glazing breakage characteristics, determine the type and thickness of window glass necessary to withstand the impact of the design missile.

The results of the study about window shutter behavior against impact of tile missile should be used to improve risk modeling of windborne debris and to improve shutter performance.

- In the experimental setup, galvanized steel panels were tested. More testing should be conducted on aluminum shutters. Further testing should be conducted on different gauge thickness of window shutters.

- Additional testing should be conducted using different types of tiles.

APPENDIX A
SAMPLE DATA WORKSHEET FOR SHINGLE MISSILE IMPACT

Table A-1. Sample data worksheet for glazing tests

Test number				
Shingle number				
Shingle damage	Yes		No	
Motor RPM				
Glass type				
Glass damage	Yes		No	
Type of glass damage	Crack		Shatter	
Shingle impact location	Width		Height	
Additional observation				

APPENDIX B
SHINGLE VELOCITY CALIBRATION AND CO-EFFICIENT OF GRIP

The wheel speed is calculated using motor RPM and its graph is given in Figure B-1. Because of the grip between the tires, the actual flight speed of the shingle is given by multiplying the wheel speed by the coefficient of grip. As mentioned earlier, the shingle velocity is calculated using a high-speed camera. The sample calculation for a full-weight new shingle at 600 RPM is given.

Parameters:

Motor RPM = 600

Wheel speed = 26.773 mph

Shingle = Full-weight new shingle

Initial time for shingle position I as per Figure B-2 A. t_1= 15:22:19.736357

Final time for shingle position II as per Figure B-2 B. t_2= 18.23.22.446019

Difference in distance traveled by shingle between time difference = 3 in

The actual distance traveled by shingle missile is different as per Figure B-3.

Using all the values, velocity of shingle at 600 RPM was calculated.

Velocity of shingle at 600 RPM = (Distance traveled) / (Final Time – Initial Time)

= (4.95in / (0.0129 sec))

= 9.747 m/sec = 21.802 mph

Once we have a value for actual shingle speed, we can relate that value with wheel speed at that RPM to get a value for the co-efficient of grip.

Coefficient of grip = (velocity of shingle at 600 RPM) / (wheel speed)

= 21.802 / (26.773)

= 0.81

The same procedure was repeated to calculate actual shingle speed at each RPM. The coefficient of grip was calculated by comparing the actual shingle speed and wheel speed for each RPM. Its average value is given as coefficient of grip (For Old/New full-weight shingle) = 0.807, and Coefficient of Grip (For Old/New half-weight shingle) = 0.934. Based on the co-efficient values, the corrected speed graph is drawn and can be seen in Figure B-4.

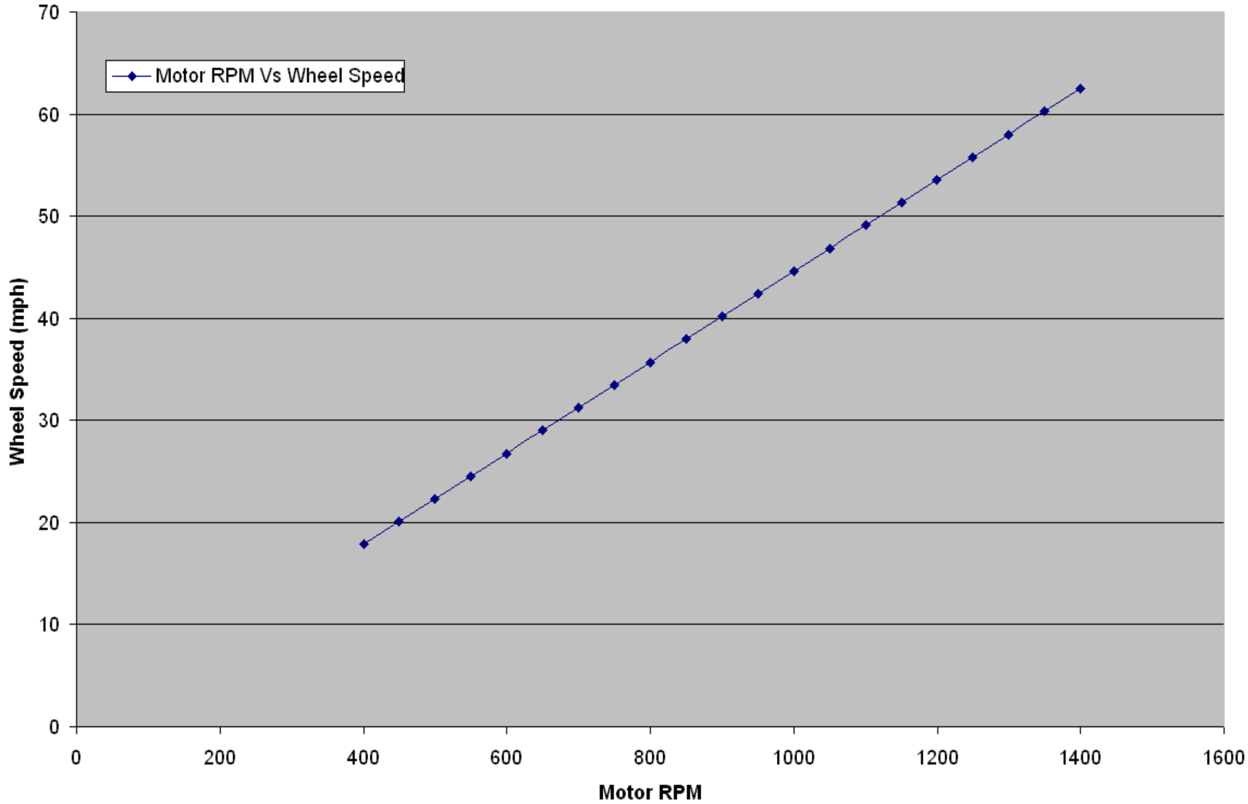

Figure B-1. Wheel speed plot corresponding to motor RPM.

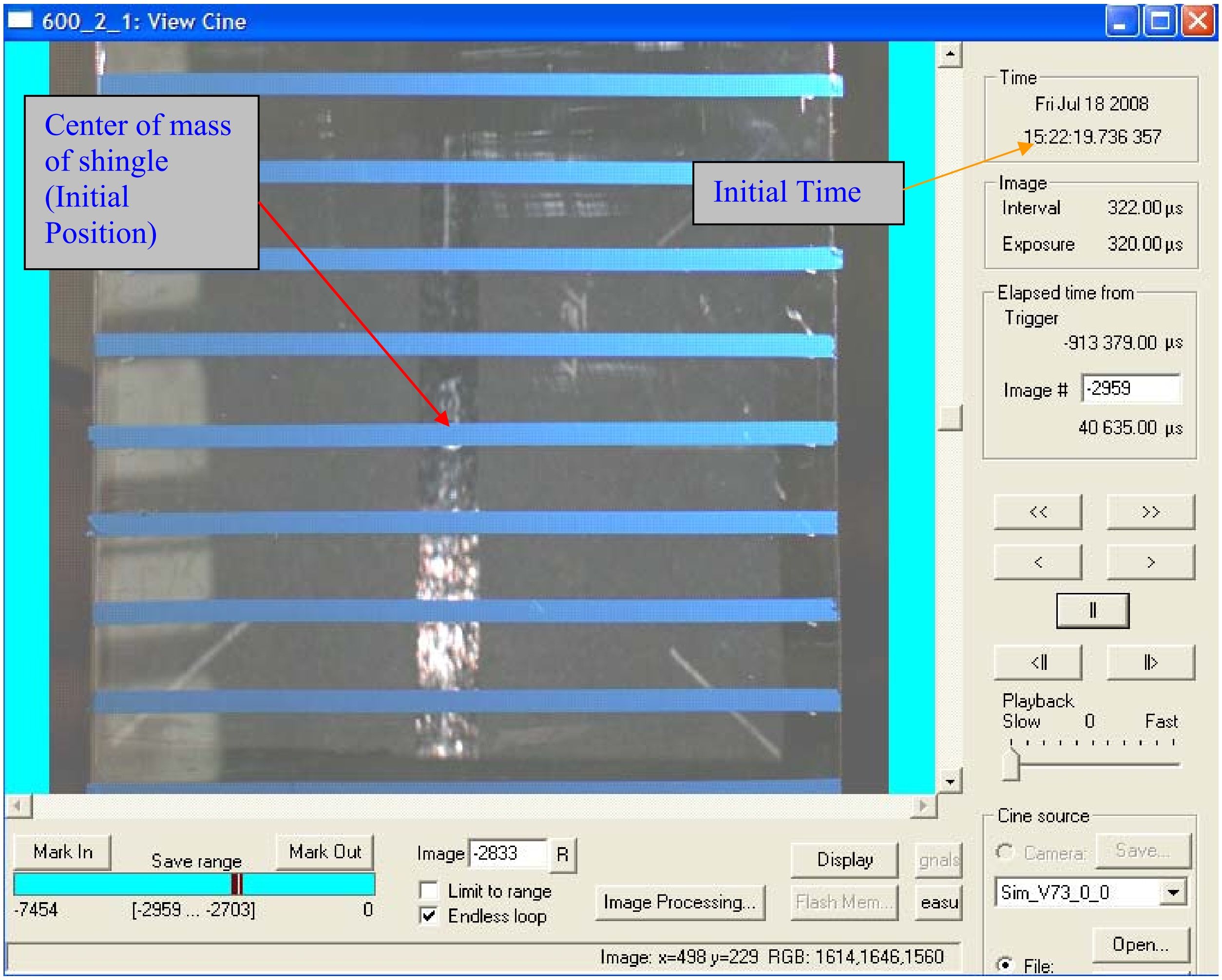

A

Figure B-2. Calibration of full weight new shingle velocity at 600 RPM. A) Typical view of shingle in high speed camera at position I. B) Typical view of shingle in high speed camera at position II.

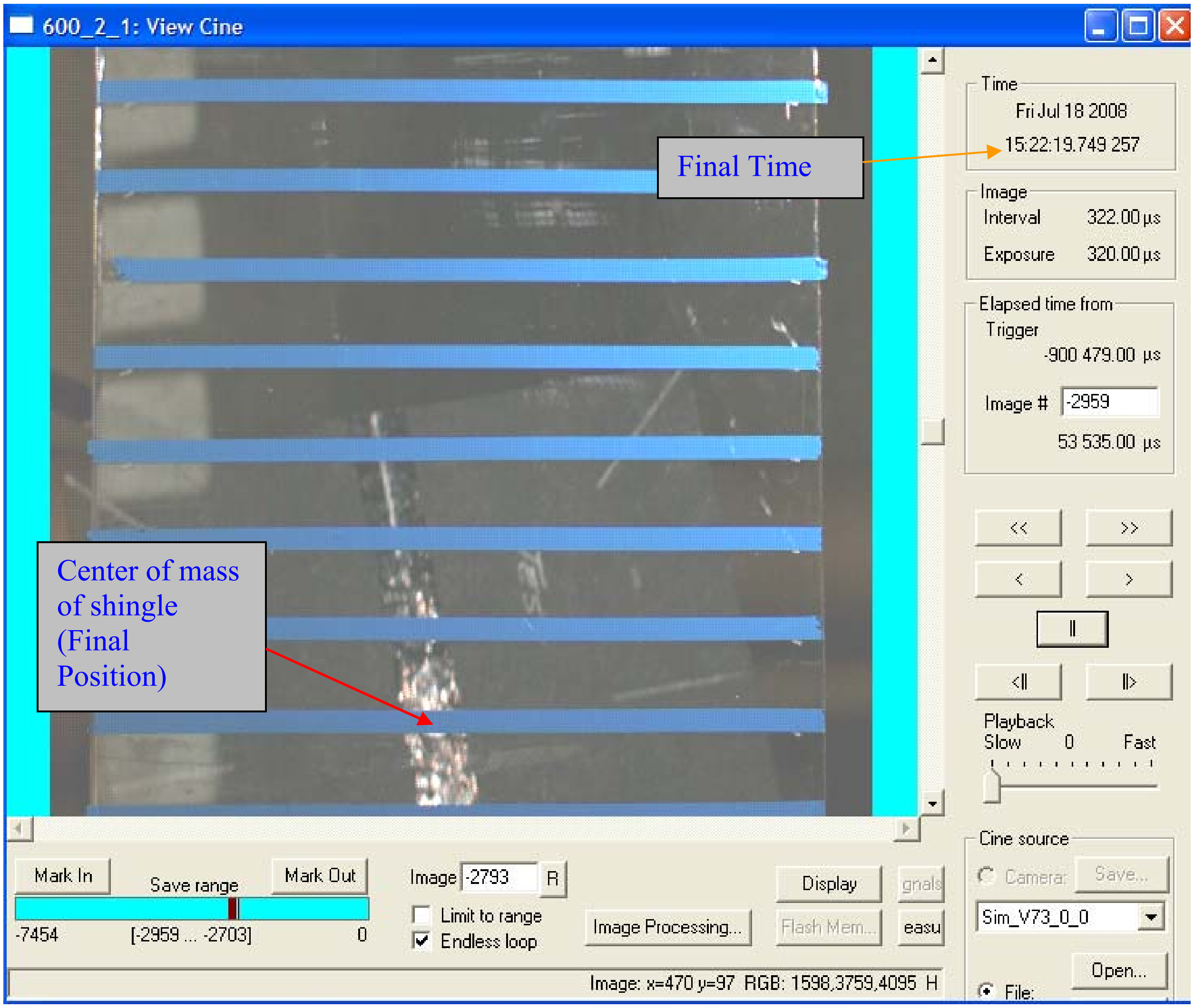

B

Figure B-2 Continued.

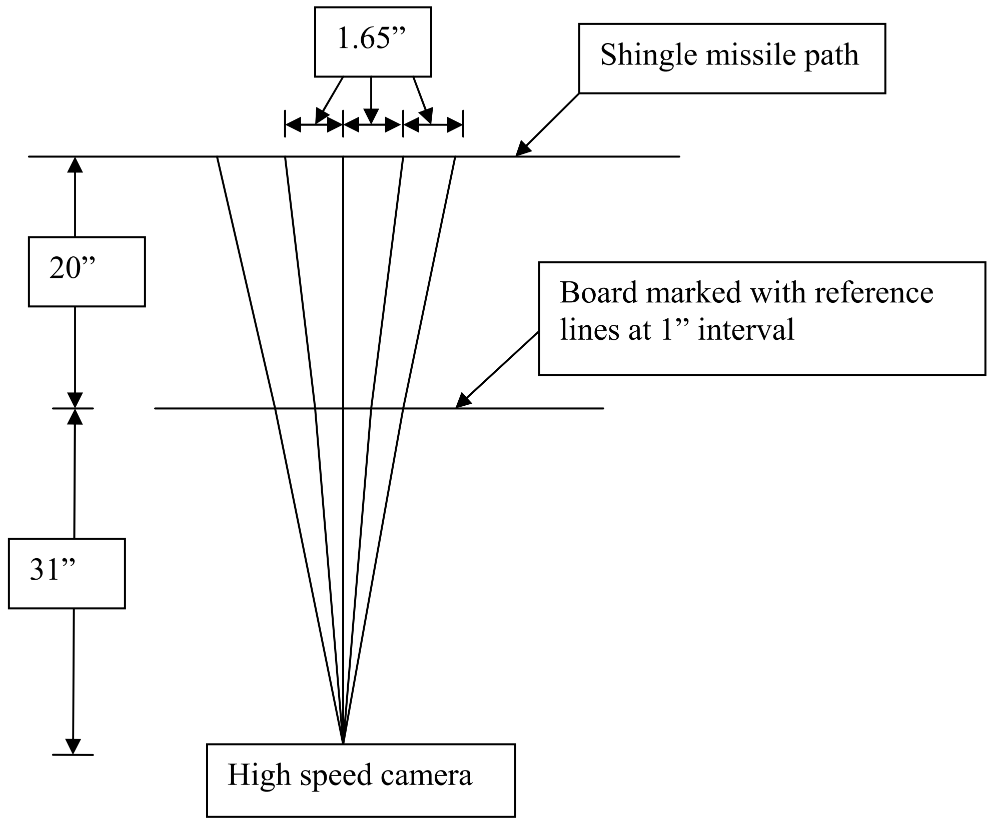

Figure B-3. Corrected distance travelled by shingle missile for 600 RPM

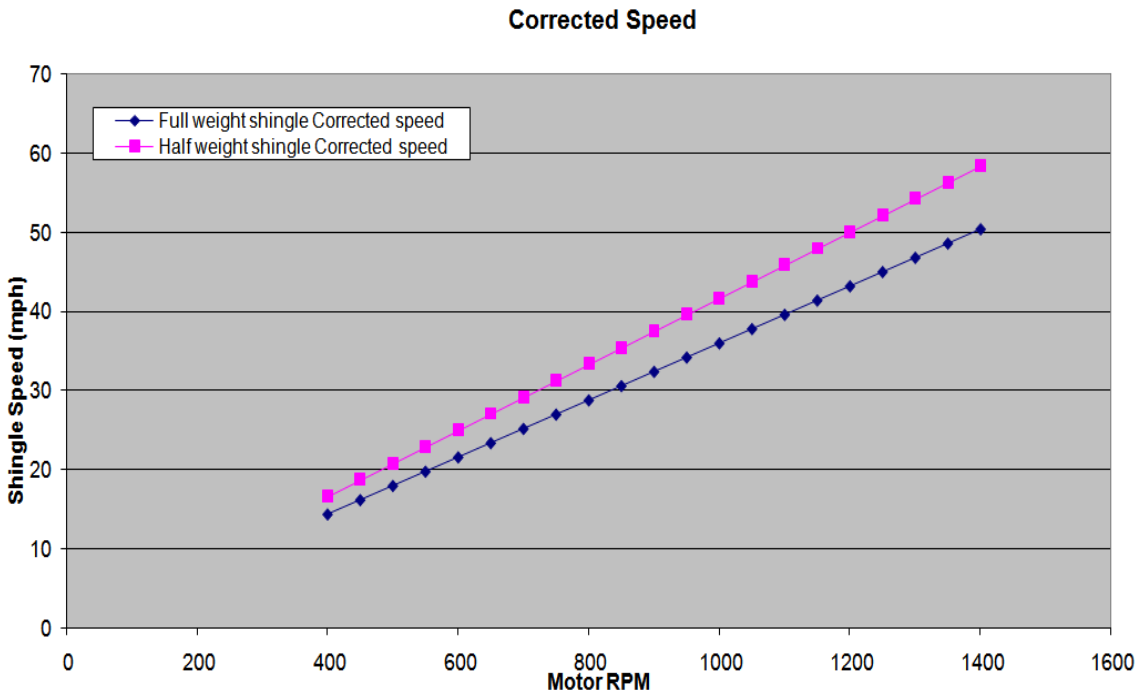

Figure B-4. Corrected shingle speed plot corresponding to motor RPM

APPENDIX C
GLASS BREAKAGE VELOCITY

The glass breakage velocity was calculated using co-efficient of grip values and given in Table C-1.

Table C-1. Glass breakage velocity

Glass breakage velocity (m/sec)						
Mode of flight – Autorotation						Tumbling
1/8” Annealed glass (2x2) Full weight new shingle	1/8” Annealed glass(2x4) Full weight new shingle	1/8” Annealed glass(2x2) Half weight new shingle	1/8” Annealed glass(2x2) Full weight old shingle	1/8” Annealed glass(2x2) Half weight old shingle	3/16” Annealed glass(2x2) Full weight new shingle	1/8” Annealed glass(2x2) Full weight new shingle
7.25	8.85	11.18	8.05	12.11	15.29	8.38
8.85	11.27	11.18	8.05	14.91	16.10	9.08
9.66	12.07	14.91	8.85	15.84	16.10	11.17
11.27	12.07	15.84	11.27	16.77	16.91	11.17
11.27	12.07	15.84	12.88	20.49	16.91	11.87
11.27	12.88	17.70	13.69	22.36	16.91	11.87
12.07	13.69	19.57	13.69	23.29	17.71	
12.88	14.49	20.49	13.69		19.32	
13.69		21.43	16.10		20.93	
13.69		22.36	16.91			
14.49		22.36	16.91			
15.29		22.36	16.91			
		23.29	18.51			
		24.22				
		24.22				

APPENDIX D
SHINGLE SIZE REDUCTION

The 3-tab shingles were cut into three full weight shingles as shown by cut marks (AA) and (BB) in Figure D-1. To make half-weight shingles, the procedure below was followed.

Average size of one shingle = 30.48 cm (12 in) X 30.48 cm (12 in)

Average weight of one shingle = 400 gm

Average size/average weight = 2.32 cm^2 /gm

To make half-weight shingle, the required area of shingle = (2.32*400)/2 = 464 cm^2

Size of the half-weight shingle = 21.54 cm (8.5 in) X 21.54 cm (8.5 in)

Full-weight shingle was cut as per dotted line shown in Figure D-2 to make a half-weight shingle.

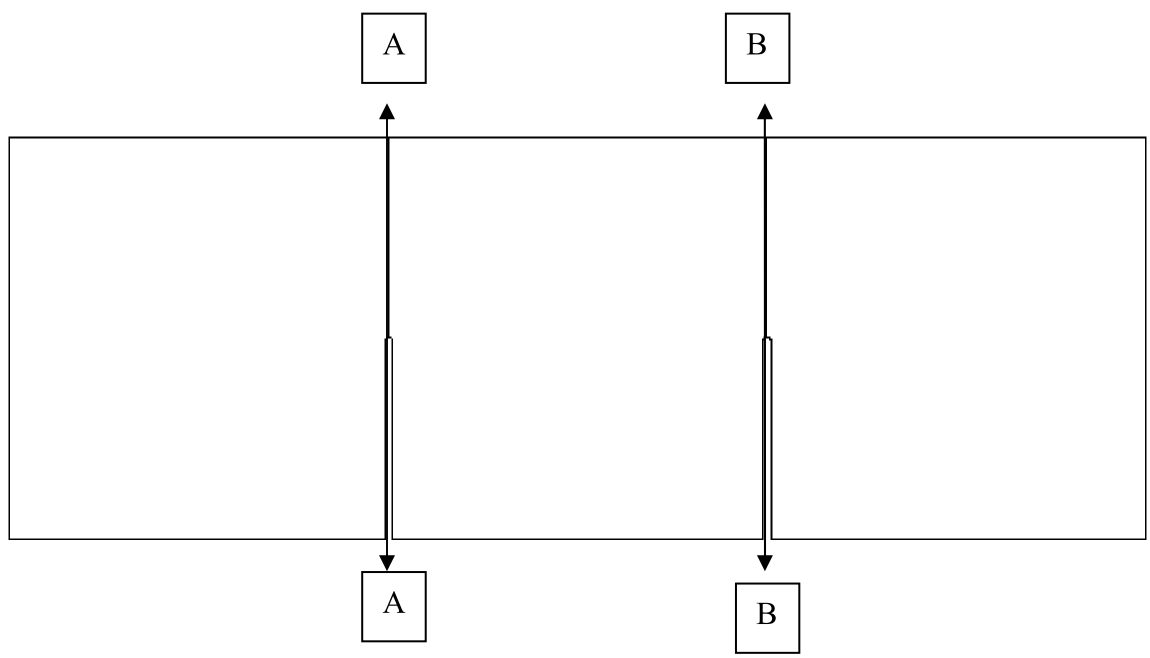

Figure D-1. Three-tab shingle.

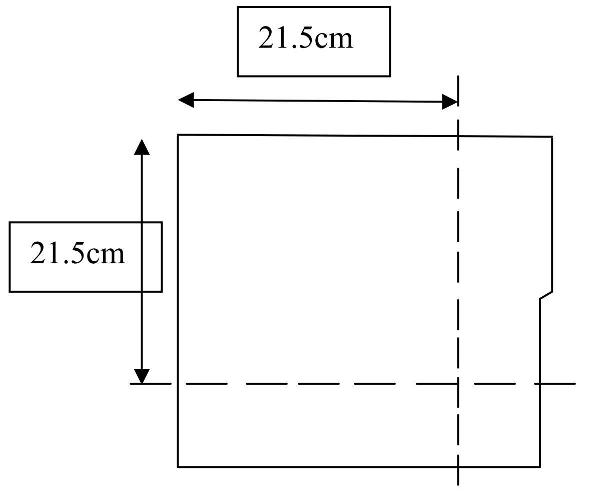

Figure D-2 Shingle size reduction.

APPENDIX E
SAMPLE DATA WORKSHEET FOR SHUTTER TESTING

Table E-1. Sample data worksheet for shutter tests

Test number								
Distance to target								
Pressure (psi)								
Missile type			Missile number					
Missile weight (kg)								
Missile dimension	Length			Width				
Damage								
H-Box								
Wing nuts/Stud								
W1	W2	W3	W4	W5	W6	W7	W8	W9
Panels								
P1	P1	P1 P2	P2	P2 P3	P3	P3 P4	P4	P4
Impact				Notes				
Location	Horizontal			Additional observations	Installation type	Type of shot		
	Vertical							
Deflection								
Number of affected panels								

APPENDIX F
MEASUREMENT OF MISSILE VELOCITY

Pressure in the Tank – 30 psi

Missile – Tile

Initial Time – 10:42:29.979646

Final Time – 10:42:29.988392

Distance travelled as per referenced line – 4 in

The actual distance travelled by missile is different due to focal length of the camera. The corrected distance factor can be calculated based on the difference of the length between the actual tile missile path and reference board with respect to camera lens. As per Figure F-1, the corrected distance factor is (1.76 – 1) = 0.76 in

Corrected distance travelled – (4*0.7692) + 4 = 7.0768 in

Velocity of tile missile = (Corrected distance) / (Final time – Initial time)

= 7.0768 / (0.008746)

= 809.147039 in/sec

= 67.42892 ft/sec = 20.55 m/sec

As shown above, for each test the corrected distance was calculated and the corresponding tile missile velocity was also calculated.

The distance travelled by the tile missile was measured for each test because of a slight variation in tank pressure. Depending upon the requirement of impact velocity, the air accumulation tank pressure was adjusted. The coefficient of variation is very small for both pressure values.

The 2x4 lumber missile velocity was measured using a radar speed gun.

Table F-1. Cannon pressure Vs tile speed

Air tank pressure (Tile launcher) (psi)	Corrected measured tile speed (m/sec)	Average speed (m/sec)	Coefficient of variation (COV)
30	20.550	20.317	2.30 %
	20.552		
	19.617		
	20.550		
21	16.599	16.445	1.87 %
	15.984		
	16.599		
	16.599		

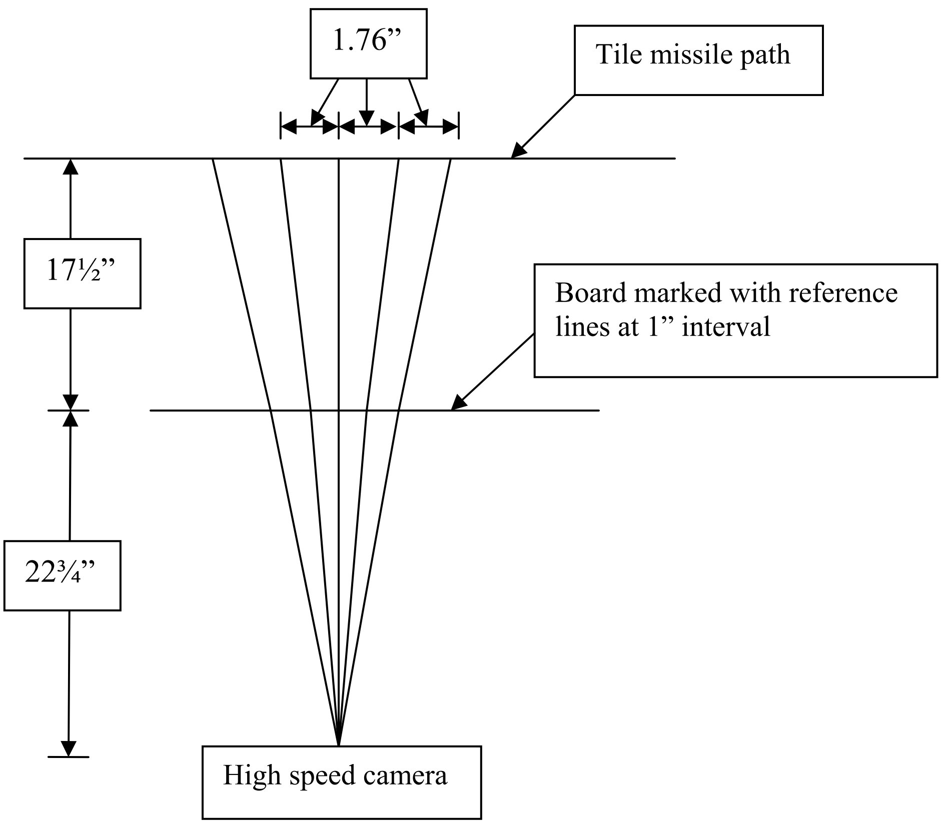

Figure F-1. Corrected distance travelled by tile missile

APPENDIX G
ONE WAY ANALYSIS OF VARIANCE (ANOVA)

When we have a single factor with several levels and multiple observations at each level, the one-way ANOVA method is useful to compare the mean difference in two or more groups. The steps for a one-way ANOVA test are performed and explained with example below.

Hypothesis

There are no differences among the different group of means. (H_0 - $\mu_1 = \mu_2$). The alternate hypothesis states that there are significant differences among them. (H_1 - $\mu_1 \neq \mu_2$).

Alpha level

$\alpha=0.05$

Example

Group X – 10,12,14,16

Group Y – 14,20,26,30

Group X – $count_x = 4$, sum = 52, average = 52/4 = 13,

Group Y – $count_y = 4$, sum = 90, average = 90/4 = 22.5,

Sum of square between group (SS_B) = $((\sum X)^2)/\ count_x + ((\sum Y)^2)/\ count_y – ((\sum T)^2)/$ Total count

$(SS_B) = (52)^2/4 + (90)^2/4 - (142)^2/8$

$(SS_B) = 180.5$

Degrees of freedom between groups (df_B) = No. of group -1 = 2-1 = 1

Sum of squares within group (SS_w) = $\{\sum X^2 – [(\sum X)^2/\ count_x]\} + \{\sum Y^2 – [(\sum Y)^2/\ count_y]\}$

$(SS_w) = (696 – 676) + (2172 – 2025)$

$(SS_w) = 167$

Degrees of freedom within group (df_w) = Total count – No. of group = 8-2 = 6

Mean square between group (MS_B) = $(SS_B)/(df_B)$ = 180.5/1 = 180.5

Mean square between group (MS_w) = (SS_w)/(df_w) = 167/6 = 27.83

F = (MS_B)/ (MS_w) = 6.49

The critical value of F at the 0.05 level, 1 degree of freedom between the groups and 6 degrees of freedom within group is

$F_{0.05}$ (1, 6) = 5.98

Write the decision rule for rejecting the null hypothesis –

Reject H_0 if $F \geq F_{Critical}$

Write the statement of results based on decision.

REFERENCES

AAMA/WDMA/CSA 101/I.S.2/A 440 “Standard specification for windows, doors and unit skylights” *American Architectural Manufacture Association*, 1827 Walden office square, Suite 550, Schaumburg, Illinois 60173-4268.

AAMA506-05 “Voluntary specification for hurricane impact and cyclic testing of fenestration products” *American Architectural Manufacture Association*, 1827 Walden office square, Suite 550, Schaumburg, Illinois 60173-4268.

ASCE 7-05 (2006). *Minimum design loads for buildings and other structures.* American Society of Civil Engineers, Reston, VA.

ASTM E1886-02 “Standard Test Method for Performance of Exterior Windows, Curtain Walls, Doors, and Storm Shutters Impacted by Missile(s) and Exposed to Cyclic Pressure Differentials”, *American Society for Testing and Materials*, 100 Barr Harbor Drive, PO Box C700, West Conshohocken, PA, 19428

ASTM E1996-99 “Standard Test Method for Performance of Exterior Windows, Curtain Walls, Doors, and Storm Shutters Impacted by wind born debris in Hurricane”, *American Society for Testing and Materials*, 100 Barr Harbor Drive, PO Box C700, West Conshohocken, PA, 19428

ASTM D3462-03 “Standard specification for Asphalt Shingles Made from Glass Felt and Surfaced with Mineral Granules”, *American Society for Testing and Materials*, 100 Barr Harbor Drive, PO Box C700, West Conshohocken, PA, 19428

Ayscue J.K. (1996), “Hurricane damage to residential structures: risk and mitigation” Retrieved October 20, 2008 from Natural Hazards Research and Applications Information Center http://www.colorado.edu/hazards/publications/wp/wp94/wp94.html

Beason, W.L. (1974). “Breakage Characteristics of Window Glass Subjected to Small Missile Impacts,” Thesis, Civil Engineering Department, Texas Tech University

Beason, W.L., Meyers, G.E., and James, R.W. (1984), “Hurricane related window glass damage in Houston”, *Journal of Structural Engineering*, Vol- 110, Issue 12, 2843-2857

Bole, S.A. (1999). “Investigations of the Mechanics of Windborne Missile Impact on Window Glass,” Thesis, Civil Engineering Department, Texas Tech University

Braden C.P. (2004). “Large wind missile impact performance of public and commercial building assemblies,” Thesis, Civil and Coastal Engineering Department, University of Florida.

Cook N.J. (1985). The designer’s guide to wind loading of building structures- Part 2, Building Research Establishment.

Federal Emergency Management Agency (FEMA). (2005a). “Mitigation Assessment Team Report: Hurricane Charley in Florida”, Rep No. FEMA 488, 5.1-5.68, Washington, D.C.

Federal Emergency Management Agency (FEMA). (2005b). “Mitigation Assessment Team Report: Hurricane Ivan in Alabama and Florida”, Rep No. FEMA 489, 5.1-5.65, Washington, D.C.

Federal Emergency Management Agency (FEMA). (2000). “Design and Construction guidance for Community Shelters”, Rep No. FEMA 361, 1-122, Washington, D.C.

Federal Emergency Management Agency (FEMA). (2000). “Hurricane Charley in Florida”, Rep No. FEMA 488,5.1-5.65, Washington, D.C.

Federal Emergency Management Agency (FEMA). (2003). “HAZUS-MH Technical Manual,” Chapter 5, Washington, D.C.

Florida Building Code (FBC). (2001). “Florida Building Code”, State of Florida, Tallahassee, FL.

Gurley, K. (2006). “Post 2004 Hurricane field survey- An evaluation of the relative performance of the Standard building code and the Florida building code”, University of Florida, 32611.

Gurley, K. (2008). “Impact of roof shingles on typical residential glass”, University of Florida, 32611.

Harris, P.L. (1978). “The Effects of Thickness and Temper on the Resistance of Glass to Small Missile Impact,” Thesis, Civil Engineering Department, Texas Tech University

Hattis, D.B. (2006). “Standards Governing Glazing Design in Hurricane Regions”, Journal of Architectural Engineering, 12(3), 108-115.

Holmes, J. D. (2002). *Wind Loading of Structures*, Spon Press, New York, NY.

International Code Council (ICC). (2006). “International Residential Code”, ICC, Falls Church, VA.

International Code Council (ICC). (2005). “ICC/NSSA Draft on Standard on the Design and Construction of Storm Shelters”, Falls Church, VA.

Krishna P. (1995). “Wind loads on low rise buildings – A review”, *Journal of Wind Engineering and Industrial Aerodynamics*, Vol- 54-55, 383-396.

Lin N. Holmes, J.D., and Letchford, C.W. (2007). “Trajectories of Wind-borne debris in horizontal winds and applications to impact testing”, Journal of Structural Engineering, Vol – 133, Issue 2, 274-282.

Meloy, Nick, Sen, Rajan, Pai, Niranjan, and Mullins, Gray, (2007). "Roof damage in new homes caused by Hurricane Charley", Journal of Structural Engineering, Vol- 21, Issue 2, 97-107.

Minor, J. (1994). "Windborne debris and building envelope." *J. Wind. Eng. Ind. Aerodyn.*, 53(1-2), 207-227.

Minor J.E. (2005), "Lessons learned from failures of the building envelope in Windstorms", *Journal of Architectural Engineering*, Vol 11, Issue 1, 10-13.

National Hurricane Center, www.nhc.noaa.gov, last updated August 2007.

NAHB Research Center (2002), "WindBorne Debris – Impact Resistant of Residential Glazing," report prepared for the U.S. Department of Housing and Urban Development, Upper Marlboro, MD.

Oliver, Clifford, and Hanson, Chris (1994), "Failure of Residential building envelopes as a result of hurricane Andrew in Dade County, Florida", Hurricanes of 1992, Ed. Ronald A Cook, Mehrdad Soltani, New York, NY, 496-508.

Pielke, R.A., and Landsea, C.W.(1998), "Normalized hurricane damages in the United States: 1925–95," *Weather and Forecasting*, Vol- 13, 621–631.

Reinhold Timothy, (2005), "Assessing the performance of Modern building codes and Standards in reducing Hurricane Damage", Retrieved July 26, 2008 from http://www.myfloridacfo.com/hurricaneinsurancetaskforce/TaskforceRS2/Appendix2/9eHurricaneInsuranceMeeting12-14-05.pdf.

Southern Building Code Congress International (SBCCI), (1994). SBCCI Test Standard For Determining Impact Resistance From Windborne Debris, SSTD 12-94, SBCCI, Inc., Birmingham, Alabama.

Stormshutters.com. "Head and Sill profiles of storm panels", Retrieved December 1, 2008 from http://www.stormshutters.com/storm-panels/profiles.html.

TAS 201-94, "Impact Test Procedures," Florida Building Code Test Protocols for High-Velocity Hurricane Zones, Department of Community Affairs Building Codes and Standards, 2555 Shumard Oak Boulevard, Tallahassee, Florida, 32399.

Unanwa, C.O., and McDonald, J.R. (2000), "Statistical analysis of Tornado generated wood missiles", *8th ASCE Speciality Conference on Probabilistic Mechanics and Structural reliability*, July 22-26, 2000, University of Notre Dame, Indiana, USA.

Wills, J. A. B., Lee, B. E., and Wyatt, T. A. (2002). “A model of windborne debris damage.” *J. Wind. Eng. Ind. Aerodyn*., 90(4–5), 555–565.

Yeatts B.B. and Mehta K.C. (1993), “Field study of internal pressures”, *Proceedings of 7th United States National Wind Engineering Conference*, June 27-30, 1993, University of California, Los Angles, USA, 889-897.

BIOGRAPHICAL SKETCH

Nirav Sunil Shah was born in Ahmedabad, India in 1985. He attended high school at Sheth C.N. Vidyalaya, Ahmedabad, India. He began his undergraduate studies at L.D. College of Engineering (Ahmedabad, Gujarat, India) in 2002. He graduated in June 2006 with his Bachelor of Engineering degree in civil engineering with distinction. After that he moved to the University of Florida at Gainesville, Florida to complete his master's degree in civil engineering with specialization in structural engineering.